




# Recent advances in multifunctional hydroxyapatite coating by electrochemical deposition

Ting-Ting Li<sup>1,2</sup>, Lei Ling<sup>1,\*</sup>, Mei-Chen Lin<sup>3,4</sup>, Hao-Kai Peng<sup>1</sup>, Hai-Tao Ren<sup>1,2</sup>,  
Ching-Wen Lou<sup>1,5,6,7,8,\*</sup>, and Jia-Horng Lin<sup>1,2,3,4,6,8,9,\*</sup> 

<sup>1</sup>Innovation Platform of Intelligent and Energy-Saving Textiles, School of Textile Science and Engineering, Tiangong University, Tianjin 300387, China

<sup>2</sup>Tianjin and Ministry of Education Key Laboratory for Advanced Textile Composite Materials, Tiangong University, Tianjin 300387, China

<sup>3</sup>School of Chinese Medicine, China Medical University, Taichung 40402, Taiwan

<sup>4</sup>Laboratory of Fiber Application and Manufacturing, Department of Fiber and Composite Materials, Feng Chia University, Taichung 40724, Taiwan

<sup>5</sup>Department of Bioinformatics and Medical Engineering, Asia University, Taichung 41354, Taiwan

<sup>6</sup>Ocean College, Minjiang University, Fuzhou 350108, China

<sup>7</sup>Department of Medical Research, China Medical University Hospital, China Medical University, Taichung 40402, Taiwan

<sup>8</sup>College of Textile and Clothing, Qingdao University, Shandong 266071, China

<sup>9</sup>Department of Fashion Design, Asia University, Taichung 41354, Taiwan

**Received:** 8 January 2020

**Accepted:** 13 February 2020

**Published online:**  
24 February 2020

© Springer Science+Business Media, LLC, part of Springer Nature 2020

## ABSTRACT

Bio-ceramic hydroxyapatite (HA) coating has been commonly used to repair the bones or as the functionalized surface of bone substitutes due to its excellent biocompatibility, superior osteo-inductivity, and great corrosion resistance. Among many other methods for synthesizing HA coating, coating via the electrochemical deposition has a high degree of crystallinity and purity, which fits the nonlinear, complex, and rugged substrates. Furthermore, HA coating can be adjusted in terms of coating morphology, thickness, and chemical component via changing the parameters, such as electrolyte ion concentration, electrolyte composition, deposition current density, and deposition time, etc. Nevertheless, the properties of electrodeposited HA coating highly pertain to the bubbles generated by water electrolysis on the substrate surface as well as the concentration polarization of electrolyte ions near the cathode during the electrodeposition process. In this study, the critical factors and mechanisms of HA coating using the electrochemical deposition method are comprehensively evaluated, thereby examining the effects of parameter optimization (i.e., current mode, ultrasonic treatment, and postprocessing). Finally, the influences of ion

Ting-Ting Li and Lei Ling have contributed equally to this work.

Address correspondence to E-mail: linglei\_tjpu@163.com; cwlou@asia.edu.tw; jhlin@fcu.edu.tw

substitution and HA composite coating on the surface structure and properties of the HA-based coatings are also discussed.

## Introduction

Hydroxyapatite ( $\text{Ca}_{10}(\text{PO}_4)_6(\text{OH})_2$ , HA or HAp) is the prime inorganic constituent of human teeth and bones and possesses good bioactivity and biocompatibility. Therefore, HA is a vital bio-ceramic materials for the bone and tooth implants in the biological clinical medicine [1–4]. Besides, due to the intrinsic osteo-inductivity, HA along with the human soft and hard tissues can form chemical bonding, which facilitates the adhesion and growth of osteoblast over the implant's surface [5–7]. HA bio-ceramics have commonly used in the bone fillers, bone scaffolds, bone cements, as well as drugs and gene delivery [8–14]. However, HA coatings possess inherent brittleness including the low tensile strength and fracture resistance, which restricts its clinical application as a non-bearing or low-load part [15–18].

In particular, the employment of HA coating can attain optimal efficacy in some biological fields [19–23]. Liu et al. proposed coating carbon fiber bio-film supported bioreactor with HA in order to strengthen the chemical durability of carbon fibers. In this case, it precluded the microorganism from flowing out and being damaged by changes in the environment [24]. In the study by Tian et al. HA coating was necessitated for magnesium metallic orthopedic implant, which could be used to manipulate the degradation velocity of magnesium. Subsequently, the implants were decomposed at bone healing speed accordingly and did not incur the inflammatory response as a result of the hydrogen corrosion in the body fluid environment [21]. Additionally, HA coating has been commonly studied as one of the surface modification strategy of bone replacing materials consisting of titanium, titanium alloy, cobalt–chromium alloy, magnesium alloy, 316 stainless steel, and C/C composites [25–29]. These materials acquired structure stability in conjunction with HA coating, preventing atoms (e.g., carbon atom and metal atom) from being released or diffused from the implant's surface so as to jeopardize the surrounding biological tissues, which in turn led to irritability and inflammation. Furthermore, HA

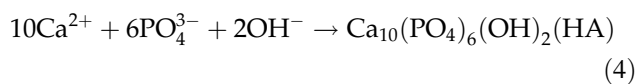
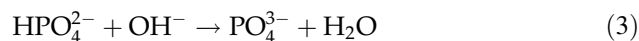
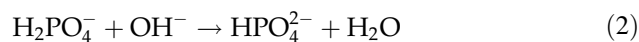
coating significantly boosted the corrosion resistance of metallic implants in the body fluid [30, 31].

The major measures used for HA coating were plasma spraying [32], RF-magnetron sputtering [33, 34], sol–gel method [35, 36], hydrothermal process [37, 38], and micro-arc oxidation [39]. Controversially, these measures could only attain HA coating with low crystallinity, unpredictable coating structure, and low adhesion with substrates [40–42]. For example, plasma spraying was the exclusive technique of coating implants that was commercially available, yet the use of a relatively higher spraying temperature rendered the coating with a mixed phase (e.g., tricalcium phosphate and calcium oxide) and higher internal residual stress [43, 44]. By contrast, the employment of RF-magnetron sputtering helped acquiring an HA coating layer with a high purity, a high bonding strength, and a great evenness over a large area, yet the target required a high production cost and is not worthy of commercial investment [45, 46]. Comparing to the aforementioned measures, electrodeposition was capable of adjusting the coating thickness, ingredient, grain size, and a microstructure over a nonlinear porous complex surface [47–49].

In this review, the performances of the electrodeposited HA coating were characterized in terms of biocompatibility, osteo-inductivity, corrosion resistance efficiency, and adhesive strength with the substrate. These properties were highly correlated with the topography, chemical component, surface roughness, and degree of crystallinity [50–55]. To gain HA coating with better properties (i.e., micro-morphology and crystallinity), the most effective method was to change the methods and conditions of electrodeposition [56, 57]. What's more, the cell performance and biological activity behavior are strongly dependent on the morphology and crystal orientation of HA coating [58–60]. Finally, the reaction mechanisms examined with electrochemical deposition of HA coating were further compared with the progress in other relative studies that have been published in the last five years.

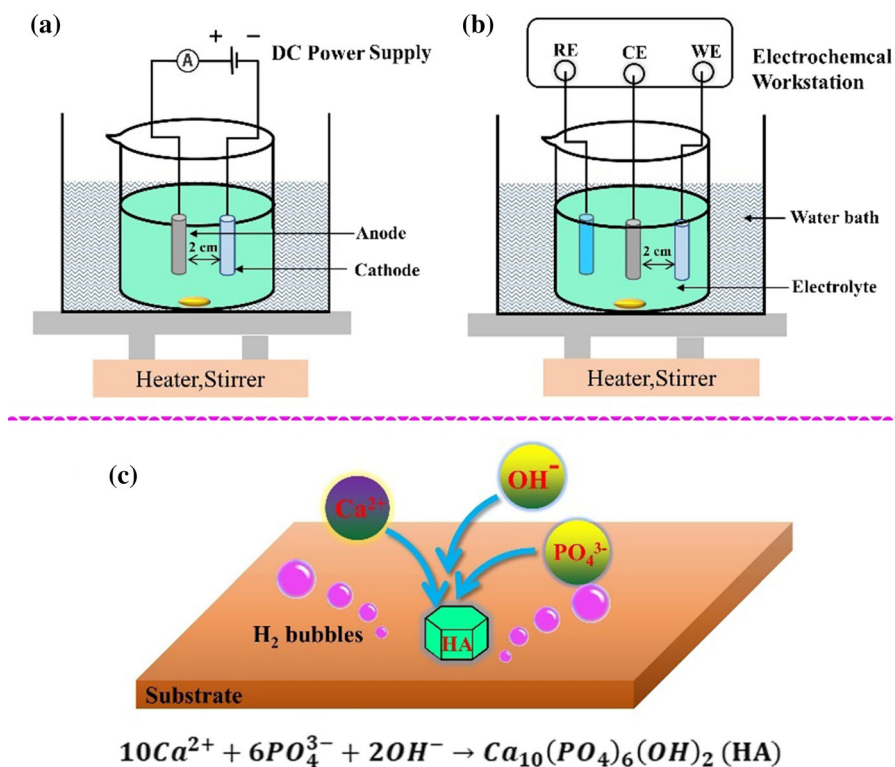
## Mechanism of HA coating by electrochemical deposition

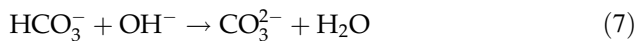
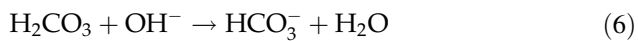
HA coating is commonly conducted using electrodeposition as follows. An aqueous solution that contains calcium ions, phosphate ions (or dihydrogen phosphate, hydrogen phosphate ions) is electrified directly. During the electrolysis, sodium or potassium is added in order to obtain a higher solution conductivity [61]. The electrodeposition system can be divided into a traditional two-electrode system and three-electrode system. The former is used for galvanostatic electrodeposition, while the latter can realize accurate potentiostatic electrodeposition precisely [62–65]. Figure 1 shows the experimental device and reaction mechanism of electrodeposition with different electrode systems. The main chemical formulae of the electrode reaction are as follows [66, 67].



In the electrodeposition process, the cathode generates bubbles and this phenomenon is consistent with Eq. (1) as the hydrogen is produced. Next, the presence of hydroxy radicals increases the pH value near the cathode. Moreover, the concentration of hydrogen phosphate and phosphate increases as a result of a rise in the hydroxide ion concentration as given in Eqs. 2 and 3. Simultaneously, calcium ions move toward the cathode and then interact with phosphate group and hydroxide, thereby generates hydroxyapatite (HA) as given in Eq. 4 [68]. Of note, characteristic peak of carbonate has been manifested by infrared spectroscopy in many studies, which suggests that the electrodeposited coating is formed by carbonated hydroxyapatite (CHA) [62]. Hence, the formation of carbonate is ascribed to carbon dioxide from the air as given in Eqs. 5, 6, and 7 [68]. For the sake of mitigating the carbonate contamination, inert gas (e.g., nitrogen) is constantly infused to the electrolyte before and during the electrodeposition [69, 70].

**Figure 1** Schematic diagram of the experimental device and reaction mechanism of electrodeposition.





In electrodeposition of HA, the electrolysis of water provides the required hydroxyl group to form hydroxyapatite and simultaneously generates a great amount of hydrogen gas bubbles [71]. A contradiction of electrodepositing HA coating between the reaction efficiency and coating quality thus arises. For instance, a rise in the current density or ion concentration helps expedite the reaction and accelerates the rate of hydroxide production considerably. Nonetheless, the more the hydroxide, the more the bubbles in the electrodeposition system. These bubbles are adsorbed over the substrate, which in turn hampers nucleation and the sequent growth of HA crystals severely. As a result, the loose and porous coating layer causes low adhesion with the substrate, which compromises the purity and crystallinity of HA coating (Fig. 1c) [69, 72]. The surface morphology, crystallinity, and crystal orientation of HA coating determine the biological properties. Accordingly, in recent years, one way to improve the biological properties and cell behavior of HA coating prepared by electrochemical deposition is to eliminate the bubbles on the substrate surface and homogenize the electrolyte ions during electrodeposition.

## Methods to improve the properties of electrodeposited HA coating

### Electrodeposition parameter optimization

As the key steps of HA coating via electrodeposition, the nucleation and growth of HA crystals are associated with deposition temperature, pH value of electrolyte, ion concentration, deposition time, and current density [65, 73–76]. A high deposition temperature is beneficial to the crystallinity, compactness, corrosion stability, and hydrophilia for HA coating [56]. To prolong the deposition time helps increase the coating thickness and influences the cell adhesion and proliferation behavior remarkably, because the variation in the deposition time may change the HA coating structure and surface morphology. The surface of HA coating with different

morphology and roughness will play an important role in the bioactivity behavior, and rough surface provides the cell and coating layer with a great contact area that facilitates the cell adhesion. However, a rough surface composed of an acicular or a flaky structure may harm the cells as it may damage the cytoderm and thus hinders the proliferation and vitality of cells [77, 78]. Similarly, the variation in pH value of electrolyte also changes the coating features [79]. Vladescu et al. focused on the flake- and needlelike morphology for HA coating. With pH = 6, the samples had higher corrosion resistance and greater in vitro biomineralization capacity, and they did not incur severe inflammation after being grafted in rats for 21 days, which suggested that the HA coating had extraordinary biocompatibility [79].

The surface morphology, coating crystallinity, and nanostructure of HA coating are heavily dependent on the current density and ion concentration. Table 1 compares current density, ion concentration, and corresponding coating characteristics that were reported in some recent studies on HA coating via electrodeposition employing a galvanostatic mode. Li et al. used ultrasonic-assisted electrodeposition to form HA coating with a current density changing from 2.5 to 7.5 mA/cm<sup>2</sup>, which resulted in a decreasing grain size from 413.65 ± 63.12 to 264.56 ± 65.33 nm (Fig. 2) [80]. In addition, with a low current density, HA crystals exhibit a retardant precipitation rate near the cathode, and thus the crystal particles grow steadily and were not subject to breakage, showing a greater crystal texture. A high current density likewise expedites the nucleation and growth rate of HA crystals, so in the later stage, the latter born crystal nucleus prevents the previously formed crystals from further growth. Based on the crystal growth theory of electrodeposition, a high current density gives rise to a comparatively higher overpotential, which in turn incurs higher depositional resistance that then facilitates the growth of the new crystal nucleus while refraining the growth of crystal particle [81, 82]. A low overpotential helps the ionic aggregation that is caused by the slow charge transfer process near the cathode. This is also beneficial to crystal growth [83, 84].

On the other hand, to optimize the electrolyte composition, such as the incorporation with hydrogen peroxide (H<sub>2</sub>O<sub>2</sub>) at different concentrations, is proven to be effective for electrodepositing HA coating. There is no hydrogen gas in the electrolytic



**Table 1** HA coating in recent studies using galvanostatic mode

Substrate	Ca <sup>2+</sup> ion concentration	Current density	Coating characteristics	Ref.
cp-Ti	0.6 mM	1.0 mA/cm <sup>2</sup>	Rodlike	2018 [85]
Carbon fibers	0.635 mM	1.0–9.0 mA	Rodlike	2018 [24]
cp-Ti	8.0 mM	15 mA/cm <sup>2</sup>	Platelike	2018 [86]
NiTi rod	8.0 mM	1.5, 3, 5 mA/cm <sup>2</sup>	Platelike	2017 [70]
cp-Ti	8.0 mM	15 mA/cm <sup>2</sup>	Platelike	2019 [20]
C/C composites	20 mM	8.0 mA/cm <sup>2</sup>	Flake-like	2019 [87]
cp-Ti	25 mM	1.0 mA/cm <sup>2</sup>	Flake-like	2018 [85]
cp-Ti	42 mM	15 mA/cm <sup>2</sup>	Needlelike	2018 [88]
Ti64	42 mM	1.25 ~ 3.61 mA/cm <sup>2</sup>	Flake-like	2015 [89]
NiTi rod	42 mM	1.5/5/15 mA/cm <sup>2</sup>	Needlelike	2017 [70]
SS316	42 mM	0.5/3.0 mA/cm <sup>2</sup>	Flake-like	2012 [69]
SS316	150 mM	5 mA/cm <sup>2</sup>	Spherical particle	2018 [90]
SS316	150 mM	10 mA/cm <sup>2</sup>	Flake-like	2018 [90]
SS316	150 mM	5/10/20 mA/cm <sup>2</sup>	Spherical particle	2019 [91]

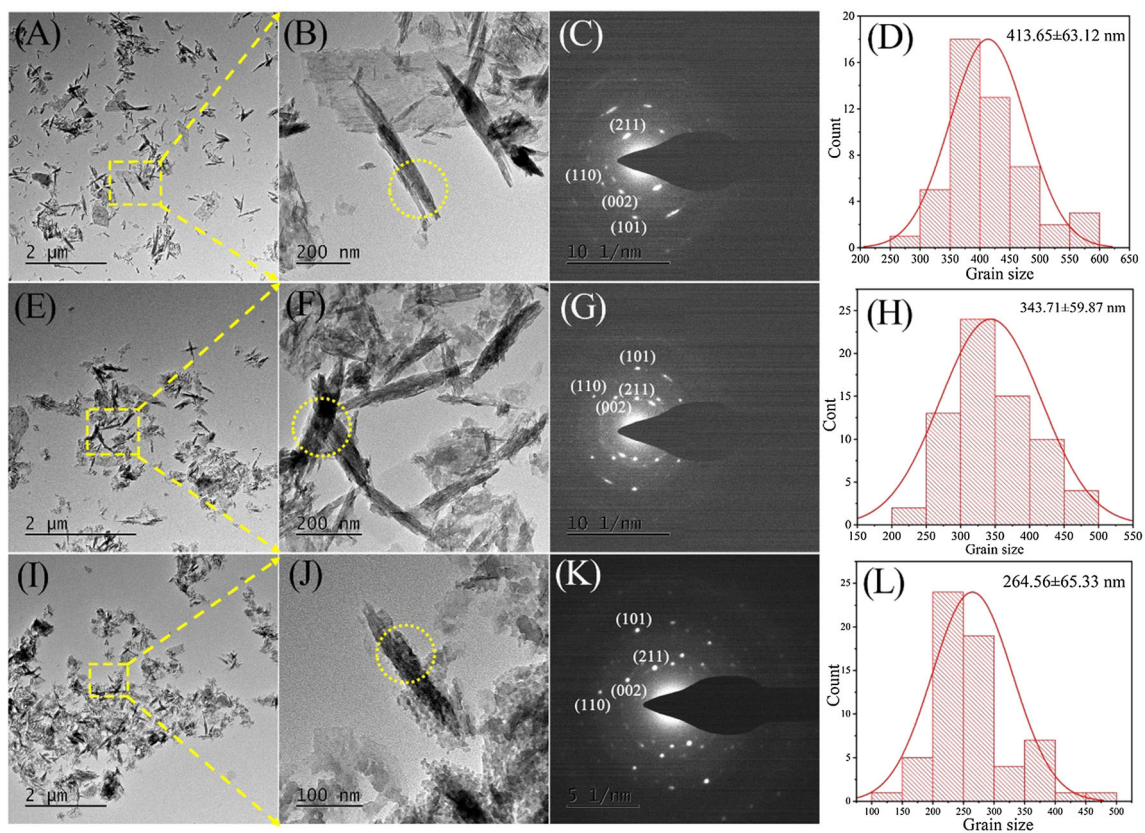


**Figure 2** Bright-field TEM image, SAED image, and particle size distribution of HA crystals under different current densities by ultrasonic-assisted electrodeposition, **a–d** 2.5 mA/cm<sup>2</sup>, **e–**

**h** 5.0 mA/cm<sup>2</sup>, and **i–l** 7.5 mA/cm<sup>2</sup> Adapted from Ref. [80], with permission from Elsevier.

product of H<sub>2</sub>O<sub>2</sub>, and the presence of H<sub>2</sub>O<sub>2</sub> at different concentrations in the electrolyte is helpful to adapt alkaline deposition conditions and eliminate

hydrogen bubbles that are detrimental to the bonding strength of HA coating layer [69]. Without H<sub>2</sub>O<sub>2</sub> in the electrolyte, the coating layer is composed of

calcium phosphate at a mixed phase, which results in a lower purity and crystallinity of HA. The electrolysis would generate more hydroxy radicals, improving the crystallinity and purity of HA coating. Li et al. found that increasing the concentration of H<sub>2</sub>O<sub>2</sub> from 0 to 4.0 ml/L transformed the electrodeposited HA crystal from being spindle-, flake-, to being wrinkle-like. The degree of crystallinity then increased from 52.34 ± 2.50 to 73.18 ± 5.75% with a significantly decreasing surface roughness that was as low as 0.877 μm (Fig. 3) [92]. Mokabber et al. examined the HA coating as related to the concentration of H<sub>2</sub>O<sub>2</sub> (i.e., 0.1, 0.5, 1.0, and 1.5 wt%) using X-ray diffraction analyses (Fig. 4). With 0.1 wt% H<sub>2</sub>O<sub>2</sub>, the deposited layer was composed of DCPD, OCP, and HA with a mixed phase. There exists an optimal concentration of hydrogen peroxide, and once it exceeds a certain threshold, calcium phosphate coating mainly consisted of HA and OCP, which made the H<sub>2</sub>O<sub>2</sub> concentration irrelevant to the composition of coating [72].

HA coating made with electrochemical deposition exhibits excellent cell adherence rates in both in vivo and in vitro cell viability assay, yet HA coating is more susceptible to dissolution as expected, indicating a low long-term stability [93]. This problem could be addressed using a hydrothermal alkali

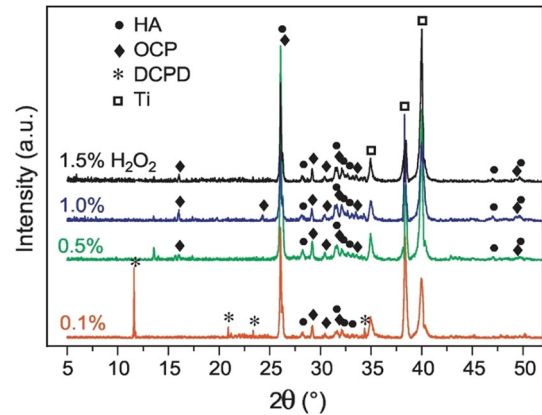


**Figure 4** XRD patterns of HA coatings deposited in 30 min at −1.4 V with various concentrations of H<sub>2</sub>O<sub>2</sub>. Adapted from Ref. [72], with permission from Elsevier.

posttreatment [87, 94, 95]. To begin with, samples are immersed coated in 80 °C 1 M sodium hydroxide for one hour, rinsed with deionized water, and dried [96]. The sodium hydroxide alkali posttreatment urges the highly soluble DCPD and β-TCP to transform into a stable calcium phosphate phase as given in Eqs. 1 and 2. Sodium ions have a smaller radius than calcium ions, which enables them to penetrate the crystalline structure. The presence of Na<sup>+</sup> in the biological apatite improves the cell adsorption capacity and bone metabolism [97].

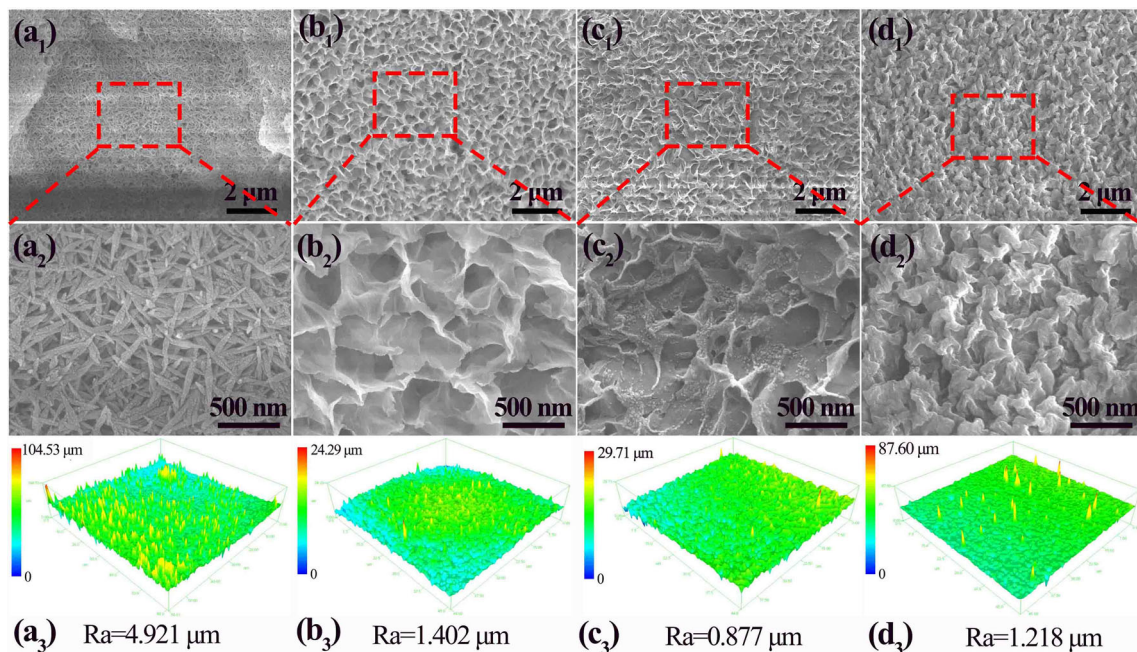
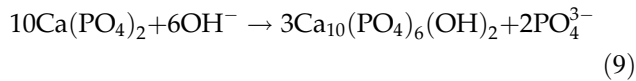
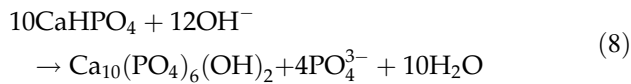


**Figure 3** SEM images and 3D profiles of electrodeposited HA coatings at different H<sub>2</sub>O<sub>2</sub> concentrations of a 0, b 0.5, c 2.0, and d 4.0 mL/L. Adapted from Ref. [92], with permission from Elsevier.





### Deposition with pulse current and pulse reverse current

The current forms utilized for electrochemical deposition of HA coating include a continuous direct current, a pulse current, and a pulse reverse current [68, 71, 91]. For the direct current deposition, suitable ion concentration of electrolyte, deposition time, and current density can avoid uneven, rough crystal texture, and surface topography that are ascribed to the electrolyte ion concentration polarization in the near the cathode [69, 98]. There are two factors for the presence of concentration polarization. One factor is that the electrolyte ions near the cathode are consumed by degrees, which prevents the ion concentration in the reacting region from being supplemented in time. The other factor is the variation in the motion tendency between the positive and negative ions in the static electric field, which leads to an excessive concentration difference in positive and negative ions.

The continuous direct current deposition generates  $\text{H}_2$  bubbles near the cathode, which blocks the mass transportation in the chemical reaction. Comparing to the direct current deposition, pulsed electrochemical deposition rather yields a HA coating layer with a greater homogeneity and better porosity [99]. The peak current density, pulse on time, and pulse off time account for the pulsed electrodeposition [100–102]. With a low current density and a long pulse off time, the pulsed electrochemical deposition is capable of increasing the coating crystallinity as well as the bonding strength between the substrate and coating layer. A sufficient pulse off time is beneficial to the growth of HA crystals, which allows the diffusion of electrolyte ions from the bulk solution to the electrode surface, which subsequently reduces the concentration polarization of the next pulse [69].

As for the direct current electrodeposition, water bath heating and magnetic stirring are used to make electrolyte ions even, avoid ion vacancy, and decrease the concentration polarization. The pulse electrodeposition makes the most of pulse off time.

When a pulse current is given, the consumed ions in the cathode/electrolyte interface can be supplemented during the pulse off time, thereby gaining a high peak current density. The intermittent reaction of the cathode is advantageous to the ion diffusion, which then reduces the concentration polarization and improves the deposition efficiency. Besides, the presence of pulse interval retards the process of crystal nucleation and epitaxial growth. At the same time, it changes the growing trend and as such prevents the occurring of abnormally structured HA crystal (Fig. 5a, b).

It is more easily obtain nanocrystalline coating of HA nanocrystals to use a pulse current than to use a direct current [103]. Using the pulse reverse electrodeposition means equivalently changing the polarity of current and as such to improve the adhesive force between the coating layer and the substrate as well as facilitate the process of electrocrystallization. Etminanfar et al. examined the electrodeposited HA coating layer over nickel–titanium superelastic alloy employing the pulse reverse electrodeposition. The pulse off time was changed to reverse current time, while the power of reverse current was only 1/30 that of a forward current. However, when the reverse duration was increased two times higher than the forward time (i.e.,  $3.0 \text{ mA/cm}^2 \cdot 1 \text{ s} \rightarrow 0.1 \text{ mA/cm}^2 \cdot 2 \text{ s}$ ), the two factors that incurred concentration polarization were successfully counteracted, and the coating layer composed of HA nano-wall was yielded afterward. The results indicated that using the pulse reverse electrodeposition helped acquire HA coating layers with ultrafine pores and a specific surface area of  $38.5 \text{ m}^2/\text{g}$ . Subsequently, the higher the reverse pulse current density, the greater the porosity [104].

During the pulse deposition, a reverse current forms unstable phase of calcium phosphate which is detrimental to the porosity and microstructure. The biggest advantage of pulse reverse electrodeposition is to outperform the electrodeposition process while efficiently assembling electrolyte with opposite charges. With the aim of this method, in situ synthesis of organic/inorganic nanoparticles is conducted, allowing the nanoparticles to attach to nanofilms or coatings [91]. The pulse reverse electrodeposition, commonly called as layer-by-layer pulse electrodeposition method (LBL-PED), is used to combine substances of different polarities in recent studies. For example, polydopamine (PDA) and HA

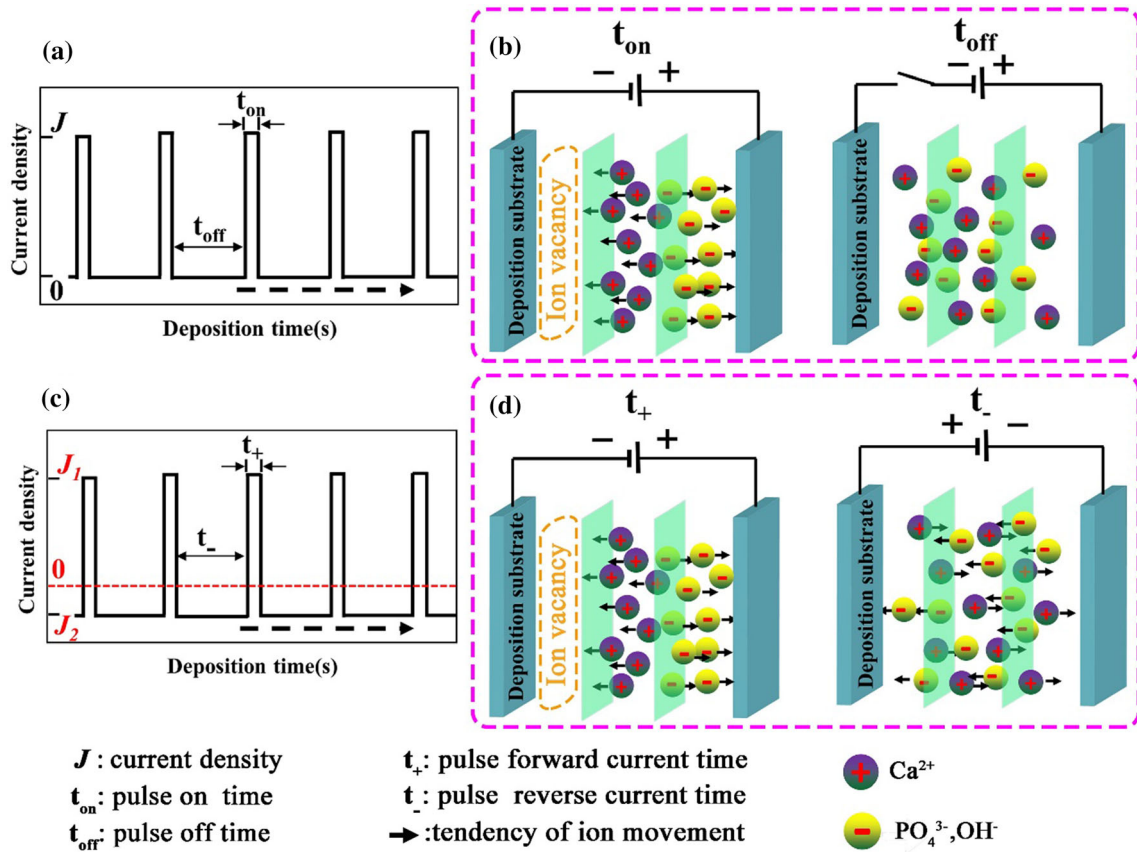


**Figure 5** Current density–time curves as well as the distribution of positive and negative ions with mechanism of reducing concentration polarization of (A/B) pulse electrodeposition and (C/D) pulse reverse electrodeposition.

are separately made by anodic deposition and cathode deposition. By means of LBL-PED method, PDA and HA are in situ synthesized by two continuous oxidation and reduction pulses so are alternatively deposited over the substrate. The employment of HA–PDA multilayered nanocoating contributes to a higher osteo-inductive activity for both in vitro and in vivo [105]. Zhou et al. employed the LBL-PED method to in situ synthesis polypyrrole-dopamine-hydroxyapatite (PPy–PDA–HA) nanofilms. The nanofilms demonstrated electroactivity, cell affinity, persistent ROS-scavenging, and osteoinduction during the production of porous Ti scaffold (Fig. 6). PPy has negative charges and is made by anodic deposition, contrary to which HA is made by cathode deposition. Hence, it is proven that LBL-PED method has a great potential in the field of tissue regeneration implants [106].

### Ultrasonic-assisted electrodeposited coating

Interacting in a liquid medium, ultrasonic waves generate a cavitation effect that can affect electrochemical reaction process and are thus commonly used in the production of nanostructured materials [107–109]. Figure 7a shows that the ultrasonic treatment is conducted during the electrodeposition process. An ultrasonic probe with an acoustic frequency of 20 kHz is positioned 30 mm away from the deposited sample near the cathode. Furthermore, the ultrasonic power of the ultrasonic probe can be manipulated in order to adjust the efficacy of electrodeposition [110]. The employment of ultrasonic treatment can significantly eliminate the presence of bubbles caused by the electrolysis of water, which in turn improves the diffusion process of electrolyte ion and makes up for the consumed ions near the cathode. As a result, HA crystals with low bond strength are removed and the coating layer is even and dense (Fig. 7b). With an ultrasonic field, bubbles can perform radial, uniform linear vibration and radiate



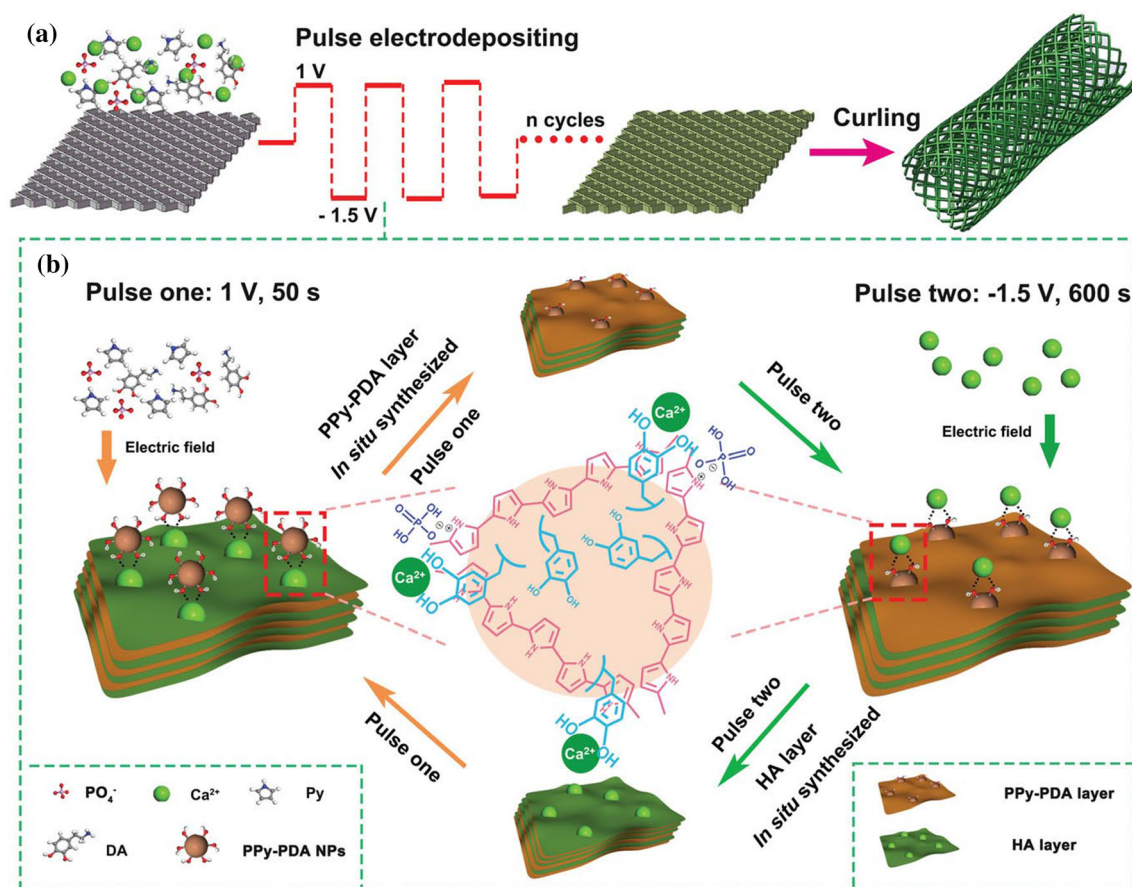


**Figure 6** PPy–PDA–HA composite nanofilm made by LBL-PED method Adapted from Ref. [106], with permission from Willey.

subordinate homogeneous spherical waves toward the electrolyte. When the bubbles move and disperse over the surface of HA microparticles in the electrolyte, the resulting homogeneous spherical waves activate the mesoscopic vortex of electrolyte, thereby attains a uniform distribution of ions and then eliminates the concentration polarization of electrolyte (Fig. 7c) [111].

With ultrasonic-assisted pulse electrodeposition, the yielded HA crystals present a denser and even needlelike structure. Without ultrasonic treatment, however, the resulting coating layer is rough and irregular needle-, flake-, or platelike calcium phosphate crystal at a mixed phase. Accordingly, Fig. 7d shows the mechanism how the ultrasonic treatment influences the electrodeposited HA crystal structure, suggesting that it precludes the possibility of intergranular agglomeration. In addition, ultrasonic waves also lead to local energy fluctuations while raising the nucleating energy required by the formation of crystals over the substrate surface, and

increasing the nucleation probability. When the substrates have an identical area, the sample group with the ultrasonic treatment forms more nucleation sites with correspondingly smaller distance among nucleation sites, which subsequently forms a more delicate microstructure ( $d_1 > d_2$ , Fig. 7d) [112].

In our latest study, the ultrasonic-assisted electrodeposition is used in order to coat a HA layer over the rugged braided structure [80]. The experimental group (i.e., conducting the ultrasonic treatment) and the control group are compared. After 7-day simulated body fluid (SBF) immersion, the experimental group acquires a smaller and more delicate apatite crystal size with a stoichiometric ratio of calcium to phosphorus (C/P ratio) being 1.59 that is close to C/P ratio of HA (1.67). This result indicates that the employment of ultrasonic treatment provides the HA coating layer with greater in vitro biomineralization and bioactivity (Fig. 8). To further analyze XRD pattern, the control group (w/o conducting the ultrasonic treatment) obtains a mixed phase of OCP and

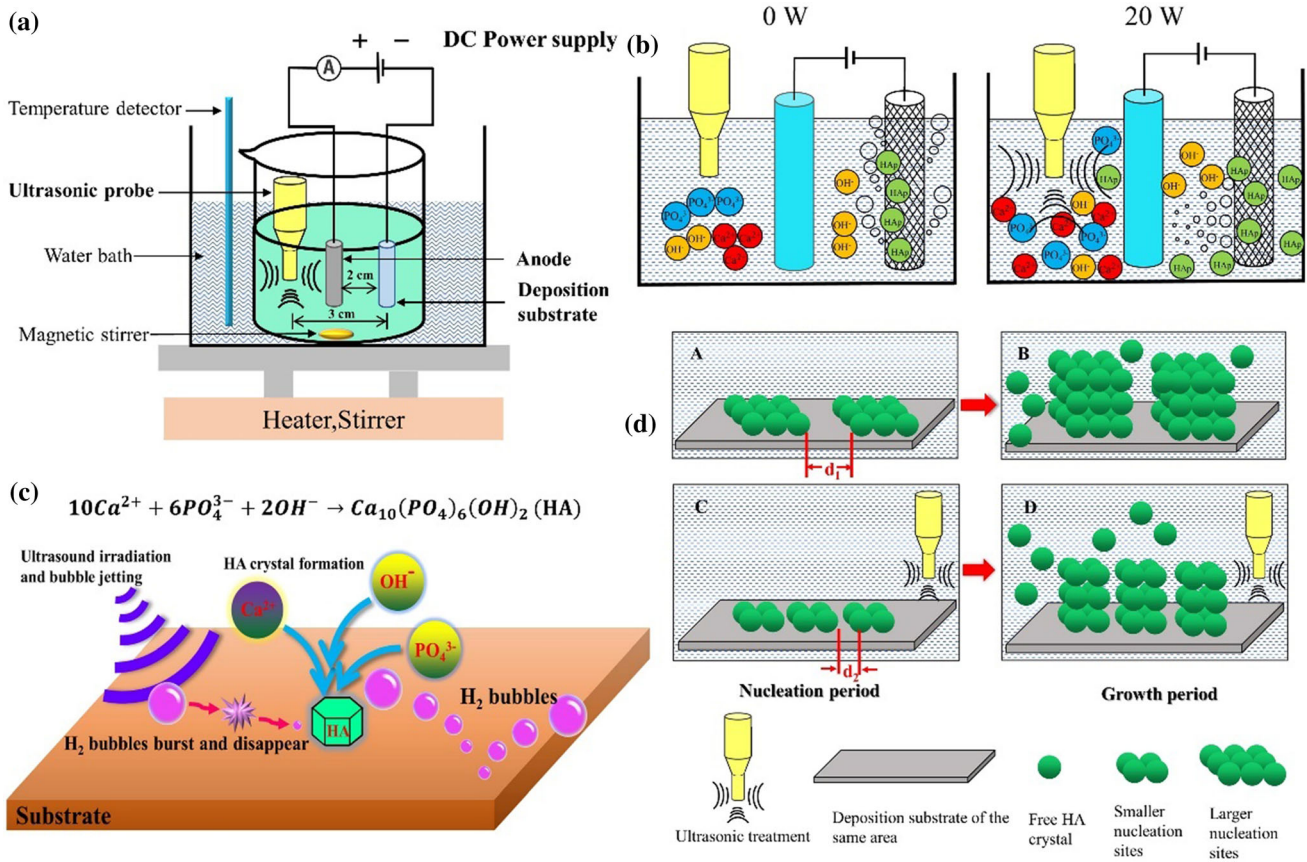


**Figure 7** Assembly and mechanism of ultrasonic-assisted electrodeposited coating Adapted from Ref. [80, 92], with permission from Elsevier.

HA as mineralization in vitro (Fig. 8f). OCP is highly soluble, which does not meet the stability requirements by orthopedic grafts [80]. The in vitro biomineralization is also called biomimetic mineralization, which means the process that in an SBF environment, the surface of materials is able to form bone-like apatite crystals [113]. In this study, bioactive HA ceramic crystal is induced into the surface of biodegradable braid scaffolds with HA crystal as the nucleation center, which incurs the polymerization of SBF ions (e.g.,  $Ca^{2+}$ ,  $OH^-$ , and  $PO_4^{3-}$ ) over the braid surface, from which apatite is precipitated. This complete process is defined as in vitro biomineralization. The results of this observation can be instructive for the biocompatibility in the further clinical application [114].

Moreover, ultrasonic waves provide HA coating with better cell adhesion capacity, facilitating the cell proliferation and differentiation. Figure 9 shows more fibroblasts adhesion and growth with ultrasonic-assisted electrodeposited coating. Namely,

ultrasonic waves increase the crystallinity of electrodeposited HA. A higher crystalline degree of HA crystals accelerates cell growth for better biological response behaviors. Besides, the surface morphology and roughness of coating layers are correlated with cell adhesion behaviors. When composed of a more densely needlelike crystal structure with a smaller surface, HA coating layer contains a greater amount of hydroxyl groups and calcium ions, which is likely to allow the coating layer to adsorb more protein that is beneficial for cell growth, which in turn facilitates the cell attachment and proliferation [86].

### HA composite coating layer

In the compact human bone are structure and composition of hydroxyapatite ceramics that include other trace elements and other functional groups (e.g.,  $CO_3^{2-}$ ,  $F^-$ ,  $Mg^{2+}$ ,  $Na^+$ ,  $K^+$ ,  $Sr^{2+}$ , and  $Zn^{2+}$ ) in addition to  $Ca^{2+}$ ,  $PO_4^{3-}$ , and  $OH^-$  [115]. In addition,



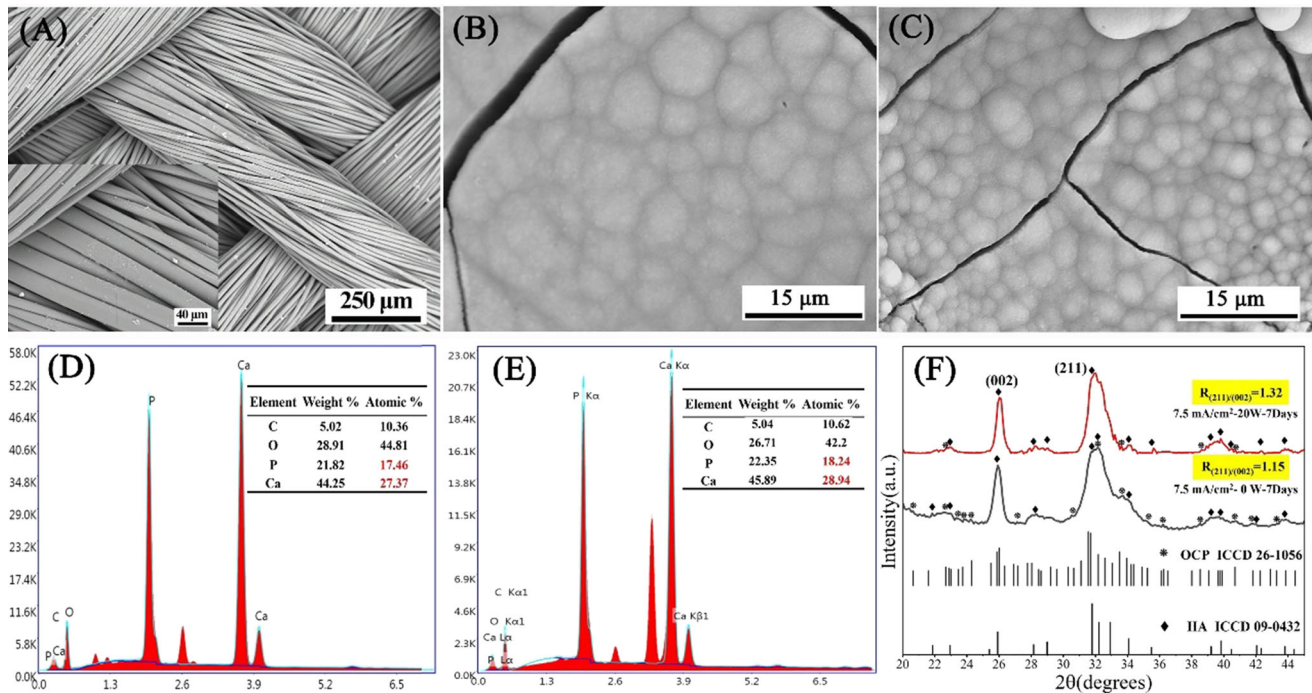
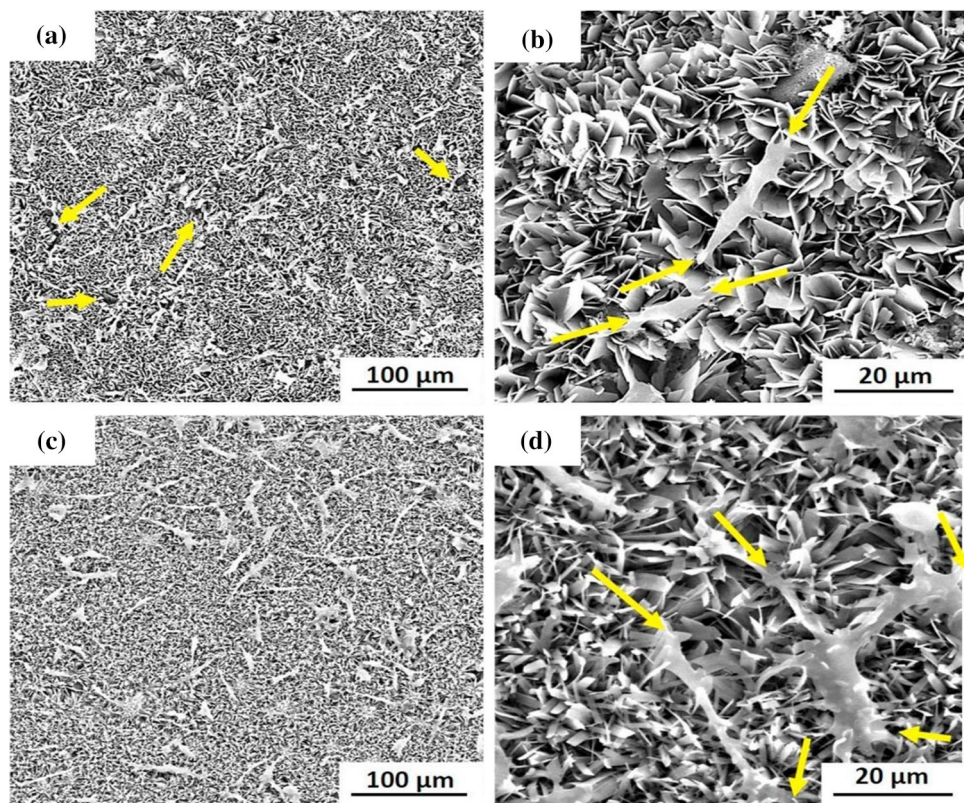


**Figure 8** SEM images and EDS analysis of 7-days immersion in SBF solution: **a** the blank group (PVA/PLA braid without electrodeposited HA), **b**, **d** 7.5 mA/cm<sup>2</sup>-0 W and **c**, **e** 7.5 mA/cm<sup>2</sup>-20 W.

(F) XRD pattern of 7-days immersion in SBF solution at 7.5 mA/cm<sup>2</sup>-20 W and 7.5 mA/cm<sup>2</sup>-0 W. Adapted from Ref. [80], with permission from Elsevier.

**Figure 9** SEM micrographs of the attached cells on **a**, **b** no ultrasonic treatment and **c**, **d** ultrasonic treatment coating. Adapted from Ref. [86], with permission from Elsevier.





bone formation ability, bone bonding strength, inflammatory response, and weak bones of the implant material surface are susceptible to the bioactive trace elements [116–119]. Therefore, many studies synthesize anion or cation substitution modified hydroxyapatite ceramics, thereby obtains higher bioactivity and biological response behaviors [120]. On the other hand, despite the acquisition of greater biocompatibility and osteo-inductivity for metallic implant materials, HA coating also helps bacteria to proliferate on the coating surface, which is why antibacterial material is required to improve the antibacterial property of HA coating [121, 122].

Due to low fracture toughness and stiffness, pure hydroxyapatite ceramics are subject to friction because of the exogenic action, which subsequently causes implanting failure. The incorporation with some functional elements or co-deposited reinforcing materials is helpful to enhance the bonding strength between HA composite coating and the substrate, anti-corrosion capability, cell adhesion and proliferation behavior, and antibacterial efficiency [123–125]. In recent years, biological multifunctional materials used for HA composite coating include metallic oxide, medical polymer, and inorganic nonmetal (e.g., zirconium dioxide, chitosan, carbon nanotube, graphene, and its derivatives) [126–131]. On one hand, these reinforcing materials can increase the specific surface area of HA coating, which helps the cells with surface adhesion, proliferation and differentiation. On the other hand, they can serve as a reinforcing medium that provides HA coating with physiological stability and mechanical property, or combines with substrate firmly, thereby improving the adhesion, adhesive strength and wear resistance, or helping protein to build signal channels over the coating surface, strengthening the cytocompatibility and antibacterial efficacy (Fig. 10) [132–135].

### **Ion-substituted HA coating**

There are two methods to complete ion-substituted HA coating. One method is to add corresponding ions to the electrolyte. During the electrodeposition process, the specified ions either are precipitating over the surface of cathode or enter the HA nanocrystalline structure. The other method is to conduct hydrothermal posttreatment to a solution containing related ions after the deposition. HA crystals have unique hexagonal structure, which

contributes possibility to multi-element ion substitution.  $\text{Ca}^{2+}$  ions are located between two unit cell locations, which provides sites to the interchange of divalent cation [138]. For example, both  $\text{Sr}^{2+}$  and  $\text{Ca}^{2+}$  have the same charge with similar ionic radius that are 1.2 Å and 1.0 Å, respectively. Hence,  $\text{Sr}^{2+}$  can be embedded into the nanocrystalline structure effectively [139].

Silver (Ag) possesses good antibacterial activity and constrains both of gram-positive and gram-negative bacterium [63, 140]. The incorporation of Ag and manganese element with HA coating can counteract the potential cytotoxicity of silver [141]. Similarly, strontium (Sr) likewise can counteract the potential cytotoxicity [142–144]. The presence of the trace active element of Sr can refrain the osteoclast activity and bone resorption while stimulating the stimulate osteoblast differentiation, which in turn reduces the fracture probability of osteoporosis patients [144]. Owing to good bactericidal performance, Sr prevents the possible inflammation [145, 146]. Besides, Sr and Ag can be evenly combined over the electrodeposited HA coating, granting the Sr/Ag/HA coating layer with more active antibacterial behavior, corrosion resistance efficiency, and biocompatibility, which subsequently stimulates the cell adhesion, cell attachment, proliferation and differentiation of MC3T3-E1 cell [142].

The trace active element of microelement silicon (Si) demonstrates indispensable functions for the growth of the human skeleton. Si accelerates connective tissue in terms of the secretion of mucopolysaccharide and collagen, and thus expedites the mineralization of new bone [147]. Si/HA coating exhibits higher bioactivity than pure HA coating and possesses a great potential application prospect of bioactive coating [87, 148]. Furthermore, Si may interfere with cell response at the implant/bone interface, which increases the bone connection between organism and the implant and speeds up the rate of bone reconstruction around Si/HA composite coating [101]. Conversely, when the body lacks of Si content, the osteoblast formation is reduced accordingly, which in turn causes skeletal abnormality [149].

Zinc (Zn) is one of the most important microelements. It strengthens the alkaline phosphatase activity, while stimulating the growth of ECM collagen and expressing sodium-dependent vitamin C transporter 2 (SVCT 2) [150]. Coating Zn/HA layer over

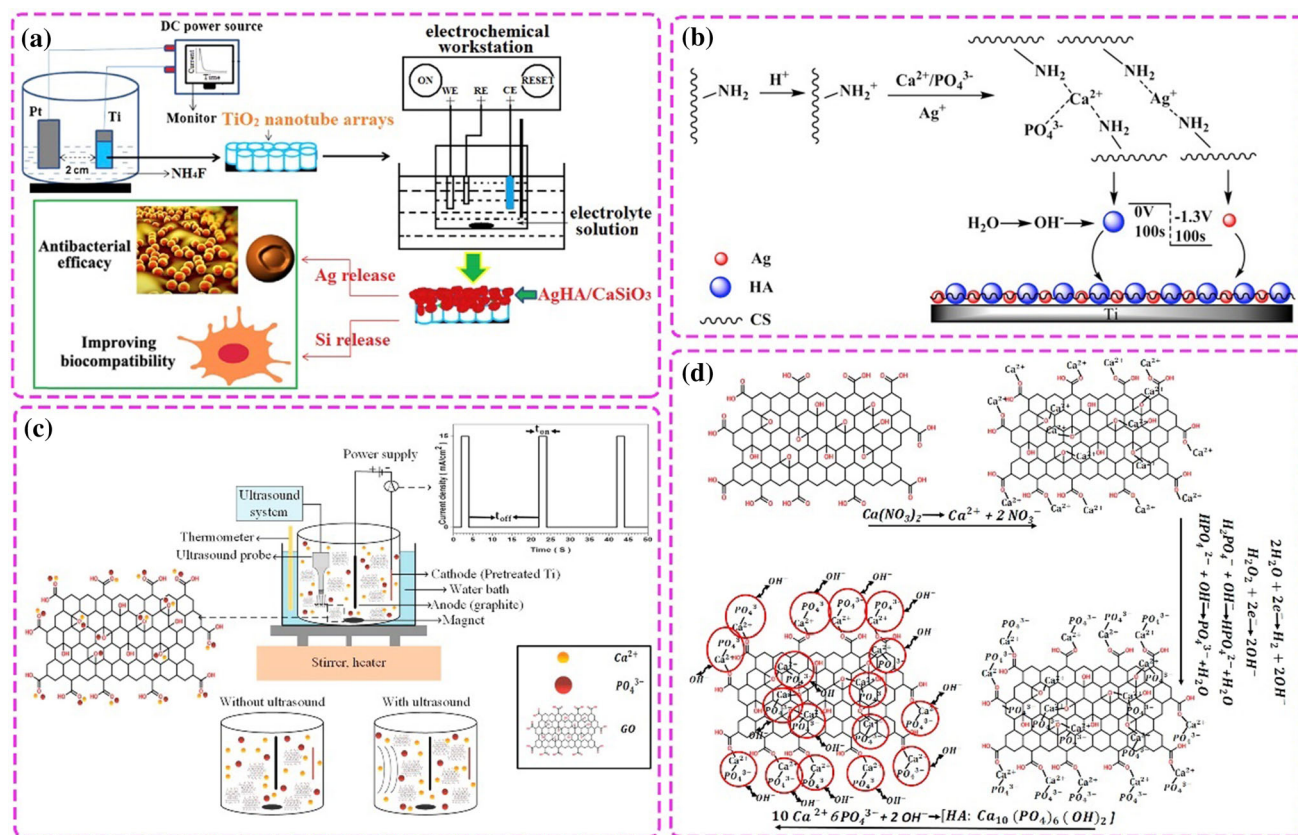


**Figure 10** Strategies for electrodepositing HA composite coating: (a) Ag/Si-HA coating Adapted from Ref. [136], with permission from Elsevier; (b) CS/HA coating Adapted from Ref. [137], with

permission from American Chemical Society, and (c, d) GO/HA electrodeposition assembly and mechanism Adapted from Ref. [110], with permission from Elsevier.

the implant surface triggers the osteoblast growth and proliferation, while reducing inflammation. The presence of Zn also causes osteoclast apoptosis. Use of Zn along with Sr prevents the occurring of osteoporosis. Zn is also proven to be antibacterial so that it hampers the growth of *streptococcus mutans*, *staphylococcus aureus*, *escherichia coli*, and *candida albicans* [151–153].

### Inorganic nonmetallic/HA composite coating

As one of the graphene derivatives, graphene oxide is a two-dimensional nanomaterial with a honeycomb structure and has extraordinary biocompatibility, mechanical property, and marginal cytotoxicity [154] [155]. It has a higher specific surface area and abundant oxygen-containing functional group (e.g., hydroxyl and carboxyl groups), which provide electrodeposited HA coating with plenty of nucleation centers that facilitate the nucleation of grains. When

applied to tissue engineering, graphene oxide is helpful to the adhesion, proliferation and differentiation of stem cells [156, 157]. With the bridging effect, graphene nanosheets can build a reinforcing network that enhances the structural stability of composite coating as well as load transfer efficiency (Fig. 10d) [158]. Fathyunes et al. used the pulsed electrochemical deposition and studied the influences of graphene oxide on the surface morphology and biological behavior of HA coating. They found that GO/HA composite coating outperformed the pure HA coating in terms of biocompatibility. This result might be ascribed to the low surface roughness and high hydrophilicity of the composite coating, which could form carbonized hydroxyapatite phase in a biological environment efficiently [159]. Xiang et al. reported that GO/HA electrodeposited coating demonstrated greater adhesive strength with the substrate ( $25.4 \pm 1.4$  MPa) when compared to pure HA coating ( $13.7 \pm 1.25$  MPa). The presence of chlorophyll could be dispersed and simultaneously functionalize

carbon nanostructure in the electrodeposition. In this case, it adjusted the integrating capacity between carbon nanocrystals and HA crystals [160]. Chakraborty et al. conducted electrodeposition to produce GO/carbon nanotubes/HA composite coating, during which chlorophyll is added as a surfactant. They acquired a greater amount of stabilized hydroxyapatite phase that provided the coating layer with greater corrosion resistance and osteo-inductivity [161].

In the natural bone, the constitutional hydroxyapatite is composed of collagen fibers that reinforce the mechanical strength and elasticity modulus of hard bone tissue. For a simulation, carbon nanotube (CNT) is added to HA coating as a reinforcing material to make most of CNT's high specific surface area, high mechanical strength, and stiffness in order to improve the abrasive resistance, fracture toughness, and long-term stability of HA coating over the implant surface [162, 163]. The presence of carbon nanotube can increase the number of nucleation sites, and thus improves the crystallinity of hydroxyapatite in the composite coating [164]. Khazeni et al. used the pulsed electrodeposition to attain CNT/HA composite coating, and the surface of magnesium alloy had a maximal crystallinity of 71.2%. Comparing to pure HA coating, composite coating separately exhibited 42% and 130% greater modulus of elasticity and hardness. The fracture toughness reached  $1.96 \pm 0.72 \text{ MPa/m}^{0.5}$  that resembled the mechanical strength of natural bones [164]. On the other hand, the failure of metallic orthopedic graft is commonly pertinent to the osteo-inductivity. Following the growth of surrounding tissue, the coating surface energy changes and the implants have a debilitated connection with surrounding bones or tissues. Chakraborty et al. also conducted pulsed electrodeposition to have composite coating of hydroxyapatite, calcium hydrophosphate and multi-walled carbon nanotubes (MWCNT) over SS316 stainless steel. The results of cell proliferation experiment proved that cells showed better uniform-ductility over the composite coating layers, rather than the bare metal implant. The electrochemical impedance spectrum (EIS) also proved that the composite coating had better corrosion resistance than the bare metal implant [165].

## Medical polymer/HA composite coating

The biomedical polymers that are used in the electrodeposited HA coating involve chitosan, gelatin, collagen, and conductive polymer, and thus can provide good biocompatibility and mechanical stability [166–171]. Chitosan is derived from chitin, and it is a natural high polymer polysaccharide with sources which is ranked only less than the sources of cellulose. Moreover, chitosan has similar glycosaminoglycan structure required by the bone mineralization for bone repair. With good biodegradability, antibacterial property, and protein affinity, chitosan as well has a great diversity of application, especially as drug delivery in the biomedicine [172]. During the electrodeposition, the addition of chitosan reinforces the adhesion between the composite coating and the substrate and can combine the good biocompatibility of HA and diverse advantages of chitosan [173–175]. When chitosan presents in the electrolyte during the electrodeposition coating of silver/HA composite, a silver-contained clathrate is formed, preventing the excessive deposition of silver elements. In addition, the electrostatic repulsion from chitosan molecules also blocks Ag nanoparticles from aggregation, causing an even distribution of silver elements (Fig. 10b) [137].

Ling et al. discovered that hydroxyapatite/nano-Ag/chitosan electrodeposited composite coating featured good antimicrobial and abrasion resistance and could adjust the  $\text{Ca}^{2+}$  and  $\text{Ag}^+$  release rate, which had a positive influence on the physiological stability of composite coating [137]. Jia et al. reported that the incorporation of  $\text{RuCl}_3$  with the electrolyte of electrodeposited HA/chitosan composite coating could refine HA grain size, fortifying the corrosion resistance of the coating layer [176]. With the aid of electrical stimulation, conductive polymer helped with the cell adhesion, proliferation and osteogenic differentiation and had a good application prospective [177, 178]. Used as an antioxidant, conductive polymers could protect cells and tissues from being damaged by excessive reactive oxygen species (ROS) [179]. Nevertheless, conductive polymers fall short of cellular affinity and osteo-inductivity and are susceptible to overoxidation. Subsequently, they loss inoxidizability and fail to gain satisfactory osteogenesis efficacy, which has engaged many scholars to explore the compensation for the composite coating



on the implant surface [106]. Polypyrrole (PPy), one of conductive polymers, possesses good in vitro and in vivo biocompatibility and can be easily synthesized to have high physical stability and body fluid resistance. The co-deposition of PPy and HA improves the corrosion resistance of the implant surface, which realizes the rapid growth of MG63 [180, 181]. Because PPy is made by anodic deposition and hydroxyapatite by cathode deposition, Chakraborty et al. employed the pulsed reverse electrochemical deposition. Monomer pyrrole was used as the raw material to in situ synthesize HA/PPy composite coating over the stainless steel. The combination of pyrrole ring's stretching effect and submicron HA ceramic matrix provided the HA/PPy composite coating with an elasticity modulus that was close to 90 GPa. Namely, the yielded elasticity modulus was between metal ( $\sim 200$  GPa) and bone (6–30 GPa) and qualified as good gradient coating [91]. Similarly, among conductive polymers, poly (3, 4-ethyl dioxophene) (PEDOT) has unique biocompatibility and doping ability, and PEDOT/HA composite coating is thus suitable for reinforcement of bonding strength between the coating and the substrates as well as for increasing coating hardness. Meanwhile, PEDOT/FHA coating provides MG63 fibroblast with an appropriate surface for adsorption and propagation, displaying greater biocompatibility than pure PEDOT coating layers [182].

## Conclusion

Hydroxyapatite has good biocompatibility, bioactivity, and osteo-inductivity. The employment of electrochemical deposition leads to a high degree of crystallinity of a nonlinear HA coating layer at a low temperature. Pure HA coating has a relatively lower elasticity modulus, fracture toughness, mechanical strength, which in turn restricts its application as implant surface. It is inevitable that electrodeposition method is accompanied by the presence of hydrogen bubbles, which adversely affects the bonding strength and surface topography of HA coating layer. The optimal HA coating can be yielded by means of optimized electrodeposition parameters, technological conditions, adjusted current form, and ultrasonic treatment. Moreover, the use of ion substitution, inorganic nonmetallic materials, medical polymers, and HA composite coating can also improve the

antibacterial property, wear resistance, and corrosion resistance of substrates, as well as the bonding strength between the coating layer and substrate significantly. In this study, summaries and comparisons are made according to the improvements in the electrodeposition, HA coating, manufacturing methods, and mechanisms. It is hoped that the proposed novel strategy makes a contribution to the bioactive ceramic coating that is used as a graft surface.

## Acknowledgements

This work is supported by the Natural Science Foundation of Tianjin (18JCQNJC03400), the Natural Science Foundation of Fujian (2018J01504, 2018J01505) and the National Natural Science Foundation of China (Grant Number 11702187). This study is also supported by the Opening Project of Green Dyeing and Finishing Engineering Research Center of Fujian University (2017001A, 2017001B, and 2017002B) and the Program for Innovative Research Team in University of Tianjin (TD13-5043).

## Compliance with ethical standards

**Conflict of interest** The authors declare that they have no conflict of interest.

## References

- [1] Alizadeh-Osgouei M, Li Y, Wen C (2019) A comprehensive review of biodegradable synthetic polymer-ceramic composites and their manufacture for biomedical applications. *Bioact Mater* 4(1):22–36
- [2] Lotsari A, Rajasekharan AK, Halvarsson M, Andersson M (2018) Transformation of amorphous calcium phosphate to bone-like apatite. *Nat Commun* 9(1):4170. <https://doi.org/10.1038/s41467-018-06570-x>
- [3] Li Z, Chu D, Gao Y, Jin L, Zhang X, Cui W, Li J (2019) Biomimicry, biomineralization, and bioregeneration of bone using advanced three-dimensional fibrous hydroxyapatite scaffold. *Mater Today Adv* 3:100014. <https://doi.org/10.1016/j.mtadv.2019.100014>
- [4] Sattar T, Manzoor T, Khalid FA, Akmal M, Saeed G (2019) Improved in vitro bioactivity and electrochemical behavior of hydroxyapatite-coated NiTi shape memory alloy. *J Mater Sci* 54(9):7300–7306. <https://doi.org/10.1007/s10853-018-03304-8>

- [5] Su Y, Cockerill I, Zheng Y, Tang L, Qin Y-X, Zhu D (2019) Biofunctionalization of metallic implants by calcium phosphate coatings. *Bioact Mater* 4:196–206
- [6] Farokhi M, Mottaghitab F, Samani S, Shokrgozar MA, Kundu SC, Reis RL, Fatahi Y, Kaplan DL (2018) Silk fibroin/hydroxyapatite composites for bone tissue engineering. *Biotechnol Adv* 36(1):68–91
- [7] Allenstein U, Selle S, Tadsen M, Patzig C, Hoeche T, Zink M, Mayr SG (2015) Coupling of metals and biominerals: characterizing the interface between ferromagnetic shape-memory alloys and hydroxyapatite. *ACS Appl Mater Interfaces* 7(28):15331–15338
- [8] Qadir M, Li Y, Wen C (2019) Ion-substituted calcium phosphate coatings by physical vapor deposition magnetron sputtering for biomedical applications: a review. *Acta Biomater* 89:14–32
- [9] Chouirfa H, Bouloussa H, Migonney V, Falentin-Daudre C (2019) Review of titanium surface modification techniques and coatings for antibacterial applications. *Acta Biomater* 83:37–54
- [10] Lai YL, Lai SB, Yen SK (2017) Paclitaxel/hydroxyapatite composite coatings on titanium alloy for biomedical applications. *Mater Sci Eng C* 79:622–628
- [11] Thomas MB, Metoki N, Mandler D, Eliaz N (2016) In situ potentiostatic deposition of calcium phosphate with gentamicin-loaded chitosan nanoparticles on titanium alloy surfaces. *Electrochim Acta* 222:355–360
- [12] Lin JH, Lee MC, Chen CK, Huang CL, Chen YS, Wen SP, Kuo ST, Lou CW (2017) Recovery evaluation of rats' damaged tibias: implantation of core-shell structured bone scaffolds made using hollow braids and a freeze-thawing process. *Mater Sci Eng C* 79:481–490
- [13] Stipnice L, Narkevica I, Sokolova M, Locs J, Ozolins J (2016) Novel scaffolds based on hydroxyapatite/poly(vinyl alcohol) nanocomposite coated porous TiO<sub>2</sub> ceramics for bone tissue engineering. *Ceram Int* 42(1):1530–1537
- [14] Goh CY, Lim SS, Tshai KY, El Azab A, Loh HS (2019) Fabrication and in vitro biocompatibility of sodium tripolyphosphate-crosslinked chitosan-hydroxyapatite scaffolds for bone regeneration. *J Mater Sci* 54(4):3403–3420. <https://doi.org/10.1007/s10853-018-3087-5>
- [15] Paul K, Lee BY, Abueva C, Kim B, Choi HJ, Bae SH, Lee BT (2017) In vivo evaluation of injectable calcium phosphate cement composed of Zn- and Si-incorporated beta-tricalcium phosphate and monocalcium phosphate monohydrate for a critical sized defect of the rabbit femoral condyle. *J Biomed Mater Res, Part B* 105(2):260–271
- [16] Kaemmerer TA, Palarie V, Schiegnitz E, Topalo V, Schroeter A, Al-Nawas B, Kaemmerer PW (2017) A biphasic calcium phosphate coating for potential drug delivery affects early osseointegration of titanium implants. *J Oral Pathol Med* 46(1):61–66
- [17] Abbasi S, Bilesan MR, Golestani-Fard F (2019) In vitro evaluation of the biocompatibility and bioactivity of plasma electrolyte oxidized titania/calcium phosphate nanocoatings on Ti. *J Mater Sci* 54(5):4277–4286. <https://doi.org/10.1007/s10853-018-3147-x>
- [18] Zhang XQ, Ma GP, Nie J, Wang Z, Wu G, Yang DZ (2018) Restorative dental resin functionalized with methacryloxy propyl trimethoxy silane to induce reversible in situ generation of enamel-like hydroxyapatite. *J Mater Sci* 53(24):16183–16197. <https://doi.org/10.1007/s10853-018-2533-8>
- [19] Baino F, Montealegre MA, Orlygsson G, Novajra G, Vitale-Brovarone C (2017) Bioactive glass coatings fabricated by laser cladding on ceramic acetabular cups: a proof-of-concept study. *J Mater Sci* 52(15):9115–9128. <https://doi.org/10.1007/s10853-017-0837-8>
- [20] Fathyunes L, Khalil-Allafi J, Moosavifar M (2019) Development of graphene oxide/calcium phosphate coating by pulse electrodeposition on anodized titanium: biocorrosion and mechanical behavior. *J Mech Behav Biomed Mater* 90:575–586
- [21] Tian Q, Lin J, Rivera-Castaneda L, Tسانhani A, Dunn ZS, Rodriguez A, Aslani A, Liu H (2019) Nano-to-submicron hydroxyapatite coatings for magnesium-based bioresorbable implants-deposition, characterization, degradation, mechanical properties, and cytocompatibility. *Sci Rep* 9(1):810. <https://doi.org/10.1038/s41598-018-37123-3>
- [22] Guan J-J, Tian B, Tang S, Ke Q-F, Zhang C-Q, Zhu Z-A, Guo Y-P (2015) Hydroxyapatite coatings with oriented nanoplate arrays: synthesis, formation mechanism and cytocompatibility. *J Mater Chem B* 3(8):1655–1666
- [23] Li N-b, Xu W-h, Zhao J-h, Xiao G-y, Lu Y-p (2018) The significant influence of ionic concentrations and immersion temperatures on deposition behaviors of hydroxyapatite on alkali- and heat-treated titanium in simulated body fluid. *Thin Solid Films* 646:163–172
- [24] Liu Q, Zhang C, Bao Y, Dai G (2018) Carbon fibers with a nano-hydroxyapatite coating as an excellent biofilm support for bioreactors. *Appl Surf Sci* 443:255–265
- [25] He D, Liu P, Liu X, Ma F, Chen X, Li W, Du J, Wang P, Zhao J (2016) Characterization of hydroxyapatite coatings deposited by hydrothermal electrochemical method on NaOH immersed Ti6Al4 V. *J Alloys Compd* 672:336–343
- [26] Poorraeisi M, Afshar A (2018) The study of electrodeposition of hydroxyapatite-ZrO<sub>2</sub>-TiO<sub>2</sub> nanocomposite coatings on 316 stainless steel. *Surf Coat Technol* 339:199–207
- [27] Liu L, Ni X-y, Xiong X-b, Ma J, Zeng X-r (2019) Low temperature preparation of SiO<sub>2</sub> reinforced hydroxyapatite

- coating on carbon/carbon composites. *J Alloys Compd* 788:768–778
- [28] Strakowska P, Beutner R, Gnyba M, Zielinski A, Scharnweber D (2016) Electrochemically assisted deposition of hydroxyapatite on Ti6Al4 V substrates covered by CVD diamond films-coating characterization and first cell biological results. *Mater Sci Eng C* 59:624–635
- [29] Kannan MB (2016) Electrochemical deposition of calcium phosphates on magnesium and its alloys for improved biodegradation performance: a review. *Surf Coat Technol* 301:36–41
- [30] Hiromoto S, Inoue M, Taguchi T, Yamane M, Ohtsu N (2015) In vitro and in vivo biocompatibility and corrosion behaviour of a bioabsorbable magnesium alloy coated with octacalcium phosphate and hydroxyapatite. *Acta Biomater* 11:520–530
- [31] Dorozhkin SV (2014) Calcium orthophosphate coatings on magnesium and its biodegradable alloys. *Acta Biomater* 10(7):2919–2934
- [32] Vu AA, Robertson SF, Ke D, Bandyopadhyay A, Bose S (2019) Mechanical and biological properties of ZnO, SiO<sub>2</sub>, and Ag<sub>2</sub>O doped plasma sprayed hydroxyapatite coating for orthopaedic and dental applications. *Acta Biomater* 92:325–335
- [33] Ivanova AA, Surmeneva MA, Surmenev RA, Depla D (2017) Structural evolution and growth mechanisms of RF-magnetron sputter-deposited hydroxyapatite thin films on the basis of unified principles. *Appl Surf Sci* 425:497–506
- [34] Ivanova AA, Surmeneva MA, Tyurin AI, Surmenev RA (2018) Correlation between structural and mechanical properties of RF magnetron sputter deposited hydroxyapatite coating. *Mater Charact* 142:261–269
- [35] Latifi SM, Fathi M, Sharifnabi A, Varshosaz J (2017) In vitro characterisation of a sol-gel derived in situ silica-coated silicate and carbonate co-doped hydroxyapatite nanopowder for bone grafting. *Mater Sci Eng C* 75:272–278
- [36] Asri RI, Harun WS, Hassan MA, Ghani SA, Buyong Z (2016) A review of hydroxyapatite-based coating techniques: sol-gel and electrochemical depositions on biocompatible metals. *J Mech Behav Biomed Mater* 57:95–108
- [37] Xia K, Pan H, Wang T, Ma S, Niu J, Xiang Z, Song Y, Yang H, Tang X, Lu W (2017) Effect of Ca/P ratio on the structural and corrosion properties of biomimetic CaP coatings on ZK60 magnesium alloy. *Mater Sci Eng C* 72:676–681
- [38] Guang S, Ke F, Shen Y (2015) Controlled preparation and formation mechanism of hydroxyapatite nanoparticles under different hydrothermal conditions. *J Mater Sci Technol* 31(8):852–856
- [39] Sedelnikova MB, Komarova EG, Sharkeev YP, Ugodchikova AV, Mushtovatova LS, Karpova MR, Sheikin VV, Litvinova LS, Khlusov IA (2019) Zn-, Cu- or Ag-incorporated micro-arc coatings on titanium alloys: properties and behavior in synthetic biological media. *Surf Coat Technol* 369:52–68
- [40] Harun WSW, Asri RIM, Alias J, Zulkifli FH, Kadrigama K, Ghani SAC, Shariffuddin JHM (2018) A comprehensive review of hydroxyapatite-based coatings adhesion on metallic biomaterials. *Ceram Int* 44(2):1250–1268
- [41] Fihri A, Len C, Varma RS, Solhy A (2017) Hydroxyapatite: a review of syntheses, structure and applications in heterogeneous catalysis. *Coord Chem Rev* 347:48–76
- [42] Fox K, Tran PA, Tran N (2012) Recent advances in research applications of nanophase hydroxyapatite. *Chem-PhysChem* 13(10):2495–2506
- [43] Ke D, Vu AA, Bandyopadhyay A, Bose S (2019) Compositionally graded doped hydroxyapatite coating on titanium using laser and plasma spray deposition for bone implants. *Acta Biomater* 84:414–423
- [44] Zheng B, Luo Y, Liao H, Zhang C (2017) Investigation of the crystallinity of suspension plasma sprayed hydroxyapatite coatings. *J Eur Ceram Soc* 37(15):5017–5021
- [45] Hamdi DA, Jiang Z-T, No K, Rahman MM, Lee P-C, Truc LNT, Kim J, Altarawneh M, Thair L, Jumaa TA-J, Dlugogorski BZ (2019) Biocompatibility study of multi-layered hydroxyapatite coatings synthesized on Ti–6Al–4 V alloys by RF magnetron sputtering for prosthetic-orthopaedic implant applications. *Appl Surf Sci* 463:292–299
- [46] Surmenev R, Surmeneva M, Grubova I, Chernozem R, Krause B, Baumbach T, Loza K, Epple M (2017) RF magnetron sputtering of a hydroxyapatite target: a comparison study on polytetrafluoroethylene and titanium substrates. *Appl Surf Sci* 414:335–344
- [47] Yilmaz E, Cakiroglu B, Gokce A, Findik F, Gulsoy HO, Gulsoy N, Mutlu O, Ozacar M (2019) Novel hydroxyapatite/graphene oxide/collagen bioactive composite coating on Ti16Nb alloys by electrodeposition. *Mater Sci Eng C* 101:292–305
- [48] Geuli O, Metoki N, Eliaz N, Mandler D (2016) Electrochemically driven hydroxyapatite nanoparticles coating of medical implants. *Adv Funct Mater* 26(44):8003–8010
- [49] Stango SAX, Karthick D, Swaroop S, Mudali UK, Vijayalakshmi U (2018) Development of hydroxyapatite coatings on laser textured 316 LSS and Ti–6Al–4V and its electrochemical behavior in SBF solution for orthopedic applications. *Ceram Int* 44(3):3149–3160



- [50] Lim S-G, Choe H-C (2019) Bioactive apatite formation on PEO-treated Ti-6Al-4V alloy after 3rd anodic titanium oxidation. *Appl Surf Sci* 484:365–373
- [51] Chen J, Zhang Z, Ouyang J, Chen X, Xu Z, Sun X (2014) Bioactivity and osteogenic cell response of TiO<sub>2</sub> nanotubes coupled with nanoscale calcium phosphate via ultrasonification-assisted electrochemical deposition. *Appl Surf Sci* 305:24–32
- [52] Khalili V, Khalil-Allafi J, Frenzel J, Eggeler G (2017) Bioactivity and electrochemical behavior of hydroxyapatite-silicon-multi walled carbon nano-tubes composite coatings synthesized by EPD on NiTi alloys in simulated body fluid. *Mater Sci Eng C* 71:473–482
- [53] Iwamoto T, Hieda Y, Kogai Y (2016) Effect of hydroxyapatite surface morphology on cell adhesion. *Mater Sci Eng C* 69:1263–1267
- [54] Khazeni D, Saremi M, Soltani R (2019) Development of HA-CNTs composite coating on AZ31 Magnesium alloy by cathodic electrodeposition. Part 2: electrochemical and in vitro behavior. *Ceram Int* 45(9):11186–11194
- [55] Spriano S, Yamaguchi S, Baino F, Ferraris S (2018) A critical review of multifunctional titanium surfaces: new frontiers for improving osseointegration and host response, avoiding bacteria contamination. *Acta Biomater* 79:1–22
- [56] Cotrut CM, Vladescu A, Dinu M, Vranceanu DM, Cotrut CM, Vladescu A, Dinu M, Vranceanu DM, Cotrut CM, Vladescu A (2018) Influence of deposition temperature on the properties of hydroxyapatite obtained by electrochemical assisted deposition. *Ceram Int* 44:669–677
- [57] D'Elia NL, Mathieu C, Hoemann CD, Laiuppa JA, Santillan GE, Messina PV (2015) Bone-repair properties of biodegradable hydroxyapatite nano-rod superstructures. *Nanoscale* 7(44):18751–18762
- [58] Chakraborty R, Seesala VS, Sengupta S, Dhara S, Saha P, Das K, Das S (2018) Comparison of osteoconduction, cytocompatibility and corrosion protection performance of hydroxyapatite-calcium hydrogen phosphate composite coating synthesized in situ through pulsed electro-deposition with varying amount of phase and crystallinity. *Surf Interfaces* 10:1–10
- [59] Huang Y, Zhou G, Zheng L, Liu H, Niu X, Fan Y (2012) Micro-/nano-sized hydroxyapatite directs differentiation of rat bone marrow derived mesenchymal stem cells towards an osteoblast lineage. *Nanoscale* 4(7):2484–2490
- [60] Costa DO, Prowse PD, Chrones T, Sims SM, Hamilton DW, Rizkalla AS, Dixon SJ (2013) The differential regulation of osteoblast and osteoclast activity by surface topography of hydroxyapatite coatings. *Biomaterials* 34(30):7215–7226
- [61] Gao JH, Guan SK, Chen J, Wang LG, Zhu SJ, Hu JH, Ren ZW (2011) Fabrication and characterization of rod-like nano-hydroxyapatite on MAO coating supported on Mg–Zn–Ca alloy. *Appl Surf Sci* 257(6):2231–2237
- [62] Bakin B, Koc Delice T, Tiric U, Birlık I, Ak Azem F (2016) Bioactivity and corrosion properties of magnesium-substituted CaP coatings produced via electrochemical deposition. *Surf Coat Technol* 301:29–35
- [63] Wang J, Gong X, Hai J, Li T (2018) Synthesis of silver-hydroxyapatite composite with improved antibacterial properties. *Vacuum* 152:132–137
- [64] Yan Y, Zhang X, Huang Y, Ding Q, Pang X (2014) Antibacterial and bioactivity of silver substituted hydroxyapatite/TiO<sub>2</sub> nanotube composite coatings on titanium. *Appl Surf Sci* 314:348–357
- [65] San H, Hu J, Zhang Y, Han J, Tang S (2019) Formation and in vitro mineralization of electrochemically deposited coatings prepared on micro-arc oxidized titanium alloy. *J Appl Electrochem* 49(5):485–501
- [66] Wu P-P, Zhang Z-Z, Xu F-J, Deng K-K, Nie K-B, Gao R (2017) Effect of duty cycle on preparation and corrosion behavior of electrodeposited calcium phosphate coatings on AZ91. *Appl Surf Sci* 426:418–426
- [67] Katić J, Metikoš-Huković M, Škapin SD, Petravić M, Varašanec M (2014) The potential-assisted deposition as valuable tool for producing functional apatite coatings on metallic materials. *Electrochim Acta* 127:173–179
- [68] Li T-T, Ling L, Lin M-C, Jiang Q, Lin Q, Lin J-H, Lou C-W (2019) Properties and mechanism of hydroxyapatite coating prepared by electrodeposition on a braid for biodegradable bone scaffolds. *Nanomaterials* 9(5):679
- [69] Gopi D, Indira J, Kavitha L (2012) A comparative study on the direct and pulsed current electrodeposition of hydroxyapatite coatings on surgical grade stainless steel. *Surf Coat Technol* 206(11–12):2859–2869
- [70] Marashi-Najafi F, Khalil-Allafi J, Etminanfar MR (2017) Biocompatibility of hydroxyapatite coatings deposited by pulse electrodeposition technique on the Nitinol superelastic alloy. *Mater Sci Eng C* 76:278–286
- [71] Chakraborty R, Sengupta S, Saha P, Das K, Das S (2016) Synthesis of calcium hydrogen phosphate and hydroxyapatite coating on SS316 substrate through pulsed electrodeposition. *Mater Sci Eng C* 69:875–883
- [72] Mokabber T, Lu LQ, van Rijn P, Vakis AI, Pei YT (2018) Crystal growth mechanism of calcium phosphate coatings on titanium by electrochemical deposition. *Surf Coat Technol* 334:526–535
- [73] Abdel-Aal EA, Dietrich D, Steinhäuser S, Wielage B (2008) Electrocrystallization of nanocrystallite calcium

- phosphate coatings on titanium substrate at different current densities. *Surf Coat Technol* 202(24):5895–5900
- [74] Schmidt R, Hoffmann V, Helth A, Gostin PF, Calin M, Eckert J, Gebert A (2016) Electrochemical deposition of hydroxyapatite on beta-Ti-40Nb. *Surf Coat Technol* 294:186–193
- [75] Liu S, Li H, Zhang L, Yin X, Guo Y (2017) In simulated body fluid performance of polymorphic apatite coatings synthesized by pulsed electrodeposition. *Mater Sci Eng C* 79:100–107
- [76] Aboudzadeh N, Dehghanian C, Shokrgozar MA (2019) Effect of electrodeposition parameters and substrate on morphology of Si-HA coating. *Surf Coat Technol* 375:341–351
- [77] Mokabber T, Zhou Q, Vakis AI, van Rijn P, Pei YT (2019) Mechanical and biological properties of electrodeposited calcium phosphate coatings. *Mater Sci Eng C* 100:475–484
- [78] Samavedi S, Whittington AR, Goldstein AS (2013) Calcium phosphate ceramics in bone tissue engineering: a review of properties and their influence on cell behavior. *Acta Biomater* 9(9):8037–8045
- [79] Vladescu A, Vranceanu DM, Kulesza S, Ivanov AN, Bramowicz M, Fedonnikov AS, Braic M, Norkin IA, Koptyug A, Kurtukova MO, Dinu M, Pana I, Surmeneva MA, Surmenev RA, Cotrut CM (2017) Influence of the electrolyte's pH on the properties of electrochemically deposited hydroxyapatite coating on additively manufactured Ti64 alloy. *Sci Rep* 7(1):16819
- [80] Li T-T, Ling L, Lin M-C, Jiang Q, Lin Q, Lou C-W, Lin J-H (2019) Effects of ultrasonic treatment and current density on the properties of hydroxyapatite coating via electrodeposition and its in vitro biomineralization behavior. *Mater Sci Eng C* 105:110062
- [81] Gamburg YD (2016) Development of the electrocrystallization theory. *Russ J Electrochem* 52(9):832–846
- [82] Budevski E, Staikov G, Lorenz WJ (2000) Electrocrystallization: nucleation and growth phenomena. *Electrochim Acta* 45(15):2559–2574
- [83] Li L, Jahanian P, Mao G (2014) Electrocrystallization of tetrathiafulvalene charge-transfer salt nanorods on gold nanoparticle seeds. *J Phys Chem C* 118(32):18771–18782
- [84] Siegfried MJ, Choi KS (2008) Elucidation of an overpotential-limited branching phenomenon observed during the electrocrystallization of cuprous oxide. *Angew Chem Int Ed Engl* 47(2):368–372
- [85] Pang SM, He Y, He P, Luo XS, Guo ZZ, Li H (2018) Fabrication of two distinct hydroxyapatite coatings and their effects on MC3T3-E1 cell behavior. *Colloids Surf B* 171:40–48
- [86] Fathyunes L, Khalil-Allafi J (2018) Effect of employing ultrasonic waves during pulse electrochemical deposition on the characteristics and biocompatibility of calcium phosphate coatings. *Ultrason Sonochem* 42:293–302
- [87] Xin-bo X, Liu L, Xin-Ye N, Jun M, Xie-rong Z (2019) Preparation of HA/Gelatin coatings on C/C composites via modified electrocrystallization/posthydrothermal treatments. *J Alloys Compd* 778:566–575
- [88] Fathyunes L, Khalil-Allafi J, Sheykholeslami SOR, Moosavifar M (2018) Biocompatibility assessment of graphene oxide-hydroxyapatite coating applied on TiO<sub>2</sub> nanotubes by ultrasound-assisted pulse electrodeposition. *Mater Sci Eng C* 87:10–21
- [89] He D-H, Wang P, Liu P, Liu X-K, Ma F-C, Zhao J (2015) HA coating fabricated by electrochemical deposition on modified Ti6Al4V alloy. *Surf Coat Technol* 277:203–209
- [90] Chakraborty R, Saha P (2018) A comparative study on surface morphology and electrochemical behaviour of hydroxyapatite-calcium hydrogen phosphate composite coating synthesized in situ through electrochemical process under various deposition conditions. *Surf Interfaces* 12:160–167
- [91] Chakraborty R, Seesala VS, Manna JS, Saha P, Dhara S (2019) Synthesis, characterization and cytocompatibility assessment of hydroxyapatite-polypyrrole composite coating synthesized through pulsed reverse electrochemical deposition. *Mater Sci Eng C* 94:597–607
- [92] Ling L, Li T-T, Lin M-C, Jiang Q, Ren H-T, Lou C-W, Lin J-H (2019) Effect of hydrogen peroxide concentration on the nanostructure of hydroxyapatite coatings via ultrasonic-assisted electrodeposition. *Mater Lett* 261:126989. <https://doi.org/10.1016/j.matlet.2019.126989>
- [93] Ahmed MK, Mansour SF, Al-Wafi R, El-dek SI, Uskokovic V (2019) Tuning the mechanical, microstructural, and cell adhesion properties of electrospun epsilon-polycaprolactone microfibers by doping selenium-containing carbonated hydroxyapatite as a reinforcing agent with magnesium ions. *J Mater Sci* 54(23):14524–14544. <https://doi.org/10.1007/s10853-019-03947-1>
- [94] Mao Z-L, Yang X-J, Zhu S-L, Cui Z-D, Li Z-Y (2015) Effect of Na<sup>+</sup> and NaOH concentrations on the surface morphology and dissolution behavior of hydroxyapatite. *Ceram Int* 41(3):3461–3468
- [95] Ouyang JL, Sun XT, Chen XS, Chen JY, Zhuang XM (2014) Preparation of layered bioceramic hydroxyapatite/sodium titanate coatings on titanium substrates using a hybrid technique of alkali-heat treatment and electrochemical deposition. *J Mater Sci* 49(4):1882–1892. <https://doi.org/10.1007/s10853-013-7879-3>

- [96] Horynová M, Remešová M, Klakurková L, Dvořák K, Ročňáková I, Yan S, Čelko L, Song G-L (2019) Design of tailored biodegradable implants: the effect of voltage on electrodeposited calcium phosphate coatings on pure magnesium. *J Am Ceram Soc* 102(1):123–135
- [97] Heimann RB (2013) Structure, properties, and biomedical performance of osteoconductive bioceramic coatings. *Surf Coat Technol* 233:27–38
- [98] Djošić MS, Panić V, Stojanović J, Mitrić M, Mišković-Stanković VB (2012) The effect of applied current density on the surface morphology of deposited calcium phosphate coatings on titanium. *Colloids Surf A* 400:36–43
- [99] Yousefi E, Sharafi S, Irannejad A (2018) The structural, magnetic, and tribological properties of nanocrystalline Fe–Ni permalloy and Fe–Ni–TiO<sub>2</sub> composite coatings produced by pulse electro co-deposition. *J Alloys Compd* 753:308–319
- [100] Seyedraoufi ZS, Mirdamadi S (2014) Effects of pulse electrodeposition parameters and alkali treatment on the properties of nano hydroxyapatite coating on porous Mg–Zn scaffold for bone tissue engineering application. *Mater Chem Phys* 148(3):519–527
- [101] Wan P, Qiu X, Tan L, Fan X, Yang K (2015) The effects of pulse electrodeposition parameters on morphology and formation of dual-layer Si-doped calcium phosphate coating on AZ31 alloy. *Ceram Int* 41(1):787–796
- [102] Li Y, Jiang H, Huang W, Tian H (2008) Effects of peak current density on the mechanical properties of nanocrystalline Ni–Co alloys produced by pulse electrodeposition. *Appl Surf Sci* 254(21):6865–6869
- [103] Vidal E, Buxadera-Palmero J, Pierre C, Manero JM, Ginebra M-P, Cazalbou S, Combes C, Rupérez E, Rodriguez D (2019) Single-step pulsed electrodeposition of calcium phosphate coatings on titanium for drug delivery. *Surf Coat Technol* 358:266–275
- [104] Etminanfar MR, Khalil-Allafi J, Parsa AB (2016) On the electrocrystallization of pure hydroxyapatite nanowalls on Nitinol alloy using a bipolar pulsed current. *J Alloys Compd* 678:549–555
- [105] Xie C, Lu X, Wang K, Yuan H, Fang L, Zheng X, Chan C, Ren F, Zhao C (2016) Pulse electrochemical driven rapid layer-by-layer assembly of polydopamine and hydroxyapatite nanofilms via alternative redox in situ synthesis for bone regeneration. *ACS Biomater Sci Eng* 2(6):920–928
- [106] Zhou T, Yan L, Xie C, Li P, Jiang L, Fang J, Zhao C, Ren F, Wang K, Wang Y, Zhang H, Guo T, Lu X (2019) A mussel-inspired persistent ROS-scavenging, electroactive, and osteoinductive Scaffold based on electrochemical-driven in situ nanoassembly. *Small* 15(25):1805440. <https://doi.org/10.1002/sml.201805440>
- [107] Bigos A, Beltowska-Lehman E, García-Lecina E, Bieda M, Szczerba MJ, Morgiel J (2017) Ultrasound-assisted electrodeposition of Ni and Ni–Mo coatings from a citrate-ammonia electrolyte solution. *J Alloys Compd* 726:410–416
- [108] Liu J, Yang L, Song Z, Xu C (2019) Microstructures and capacitance performance of MnO<sub>2</sub> films fabricated by ultrasonic-assisted electrodeposition. *Appl Surf Sci* 478:94–102
- [109] Nevers A, Hallez L, Touyeras F, Hihn JY (2018) Effect of ultrasound on silver electrodeposition: crystalline structure modification. *Ultrason Sonochem* 40(Pt B):60–71
- [110] Fathyunes L, Khalil-Allafi J (2017) Characterization and corrosion behavior of graphene oxide-hydroxyapatite composite coating applied by ultrasound-assisted pulse electrodeposition. *Ceram Int* 43(16):13885–13894
- [111] Walker CT, Walker R (1973) Effect of ultrasonic agitation on some properties of electrodeposits. *Electrodepos Surf Treat* 1(6):457–469
- [112] Tudela I, Zhang Y, Pal M, Kerr I, Cobley AJ (2014) Ultrasound-assisted electrodeposition of composite coatings with particles. *Surf Coat Technol* 259:363–373
- [113] Akiva A, Kerschnitzki M, Pinkas I, Wagermaier W, Yaniv K, Fratzi P, Addadi L, Weiner S (2016) Mineral formation in the larval zebrafish tail bone occurs via an acidic disordered calcium phosphate phase. *J Am Chem Soc* 138(43):14481–14487
- [114] Zheng T, Wu C, Zhang Y, Chen M, Cummings PT (2018) Molecular investigation of the initial nucleation of calcium phosphate on TiO<sub>2</sub> substrate: the effects of surface nanotopographies. *Cryst Growth Des* 18(6):3283–3290
- [115] Okada M, Furuzono T (2012) Hydroxylapatite nanoparticles: fabrication methods and medical applications. *Sci Technol Adv Mater* 13(6):064103. <https://doi.org/10.1088/1468-6996/13/6/064103>
- [116] Shen S, Cai S, Bao X, Xu P, Li Y, Jiang S, Xu G (2018) Biomimetic fluoridated hydroxyapatite coating with micron/nano-topography on magnesium alloy for orthopaedic application. *Chem Eng J* 339:7–13
- [117] Rau JV, Fosca M, Cacciotti I, Laureti S, Bianco A, Teghil R (2013) Nanostructured Si-substituted hydroxyapatite coatings for biomedical applications. *Thin Solid Films* 543(24):167–170
- [118] Neacsu IA, Stoica AE, Vasile BS, Andronescu E (2019) Luminescent hydroxyapatite doped with rare earth elements for biomedical applications. *Nanomaterials* 9(2):239. <https://doi.org/10.3390/nano9020239>
- [119] Guo X, Long YP, Li WQ, Dai HL (2019) Osteogenic effects of magnesium substitution in nano-structured beta-tricalcium phosphate produced by microwave synthesis.



- J Mater Sci 54(16):11197–11212. <https://doi.org/10.1007/s10853-019-03674-7>
- [120] Cacciotti I (2019) Multisubstituted hydroxyapatite powders and coatings: the influence of the codoping on the hydroxyapatite performances. *Int J Appl Ceram Technol* 16:1864–1884
- [121] Kurtjak M, Vukomanović M, Krajnc A, Kramer L, Turk B, Suvorov D (2016) Designing Ga(iii)-containing hydroxyapatite with antibacterial activity. *RSC Adv* 6(114):112839–112852
- [122] Huang Y, Zhang XJ, Zhao RL, Mao HH, Yan YJ, Pang XF (2015) Antibacterial efficacy, corrosion resistance, and cytotoxicity studies of copper-substituted carbonated hydroxyapatite coating on titanium substrate. *J Mater Sci* 50(4):1688–1700. <https://doi.org/10.1007/s10853-014-8730-1>
- [123] Vladescu A, Padmanabhan SC, Ak Azem F, Braic M, Titorencu I, Birlık I, Morris MA, Braic V (2016) Mechanical properties and biocompatibility of the sputtered Ti doped hydroxyapatite. *J Mech Behav Biomed Mater* 63:314–325
- [124] Ciobanu G, Harja M (2019) Cerium-doped hydroxyapatite/collagen coatings on titanium for bone implants. *Ceram Int* 45(2):2852–2857
- [125] Rau JV, Cacciotti I, Bonis AD, Fosca M, Komlev VS, Latini A, Santagata A, Teghil R (2014) Fe-doped hydroxyapatite coatings for orthopedic and dental implant applications. *Appl Surf Sci* 307(307):301–305
- [126] Lahiri D, Ghosh S, Agarwal A (2012) Carbon nanotube reinforced hydroxyapatite composite for orthopedic application: a review. *Mater Sci Eng C* 32(7):1727–1758
- [127] Medeiros JS, Oliveira AM, Carvalho JOD, Ricci R, Martins MDCC, Rodrigues BVM, Webster TJ, Viana BC, Vasconcelos LMR, Canevari RA, Marciano FR, Lobo AO (2018) Nanohydroxyapatite/graphene nanoribbons nanocomposites induce in vitro osteogenesis and promote in vivo bone neof ormation. *ACS Biomater Sci Eng* 4:1580–1590
- [128] Sabzi M, Far SM, Dezf uli SM (2018) Characterization of bioactivity behavior and corrosion responses of hydroxyapatite-ZnO nanostructured coating deposited on NiTi shape memory alloy. *Ceram Int* 44(17):21395–21405
- [129] Kollath VO, Chen Q, Mullens S, Luyten J, Traina K, Boccaccini AR, Cloots R (2016) Electrophoretic deposition of hydroxyapatite and hydroxyapatite-alginate on rapid prototyped 3D Ti6Al4V scaffolds. *J Mater Sci* 51(5):2338–2346. <https://doi.org/10.1007/s10853-015-9543-6>
- [130] Lian H, Liu X, Meng ZX (2019) Enhanced mechanical and osteogenic differentiation performance of hydroxyapatite/zein composite for bone tissue engineering. *J Mater Sci* 54(1):719–729. <https://doi.org/10.1007/s10853-018-2796-0>
- [131] Zhao SN, Yang DL, Wang D, Pu Y, Le Y, Wang JX, Chen JF (2019) Design and efficient fabrication of micro-sized clusters of hydroxyapatite nanorods for dental resin composites. *J Mater Sci* 54(5):3878–3892. <https://doi.org/10.1007/s10853-018-3125-3>
- [132] Fu Q-G, Gu C-G, Li H-J, Chu Y-H, Lu J-H, Zhang L-L (2013) Microstructure and mechanical properties of SiC nanowires reinforced hydroxyapatite coating on carbon/carbon composites. *Mater Sci Eng, A* 563:133–137
- [133] Avcu E, Baştan FE, Abdullah HZ, Rehman MAU, Avcu YY, Boccaccini AR (2019) Electrophoretic deposition of chitosan-based composite coatings for biomedical applications: a review. *Prog Mater Sci* 103:69–108
- [134] Leilei Z, Hejun L, Kezhi L, Shouyang Z, Qiangang F, Yulei Z, Jinhua L, Wei L (2014) Preparation and characterization of carbon/SiC nanowire/Na-doped carbonated hydroxyapatite multilayer coating for carbon/carbon composites. *Appl Surf Sci* 313:85–92
- [135] Michiardi A, Helary G, Nguyen PCT, Gamble LJ, Anagnostou F, Castner DG, Migonney V (2010) Bioactive polymer grafting onto titanium alloy surfaces. *Acta Biomater* 6(2):667–675
- [136] Huang Y, Xu Z, Zhang X (2017) Nanotube-formed Ti substrates coated with silicate/silver co-doped hydroxyapatite as prospective materials for bone implants. *J Alloys Compd* 697:182–199
- [137] Yan L, Xiang Y, Yu J, Wang Y, Cui W (2017) Fabrication of antibacterial and antiwear hydroxyapatite coatings via in situ chitosan-mediated pulse electrochemical deposition. *ACS Appl Mater Interfaces* 9(5):5023–5030
- [138] Wei Q, Wang Y, Li X, Yang M, Chai W, Wang K, Zhang Y (2016) Study the bonding mechanism of binders on hydroxyapatite surface and mechanical properties for 3DP fabrication bone scaffolds. *J Mech Behav Biomed Mater* 57:190–200
- [139] Sekine Y, Motokawa R, Kozai N, Ohnuki T, Matsumura D, Tsuji T, Kawasaki R, Akiyoshi K (2017) Calcium-deficient hydroxyapatite as a potential sorbent for strontium. *Sci Rep* 7(1):2064. <https://doi.org/10.1038/s41598-017-02269-z>
- [140] Anjaneyulu U, Priyadarshini B, Grace AN, Vijayalakshmi U (2017) Fabrication and characterization of Ag doped hydroxyapatite-polyvinyl alcohol composite nanofibers and its in vitro biological evaluations for bone tissue engineering applications. *J Sol-Gel Sci Technol* 81(3):1–12
- [141] Huang Y, Wang W, Zhang X, Liu X, Xu Z, Han S, Su Z, Liu H, Gao Y, Yang H (2018) A prospective material for orthopedic applications: ti substrates coated with a composite coating of a titania-nanotubes layer and a silver-

- manganese-doped hydroxyapatite layer. *Ceram Int* 44(5):5528–5542
- [142] Huang Y, Zhang X, Zhang H, Qiao H, Zhang X, Jia T, Han S, Gao Y, Xiao H, Yang H (2017) Fabrication of silver- and strontium-doped hydroxyapatite/TiO<sub>2</sub> nanotube bilayer coatings for enhancing bactericidal effect and osteoinductivity. *Ceram Int* 43(1):992–1007
- [143] Lowry N, Brolly M, Han Y, McKillop S, Meenan BJ, Boyd AR (2018) Synthesis and characterisation of nanophase hydroxyapatite co-substituted with strontium and zinc. *Ceram Int* 44(7):7761–7770
- [144] Morejón-Alonso L, Mochales C, Nascimento L, Müller W-D (2019) Electrochemical deposition of Sr and Sr/Mg-co-substituted hydroxyapatite on Ti-40Nb alloy. *Mater Lett* 248:65–68
- [145] Yuan Q, He L, Qian ZJ, Zhou C, Hong P, Wang Z, Wang Y, Sun S, Li C (2018) Significantly accelerated osteoblast cell growth on TiO<sub>2</sub>/SrHA composite mediated by phenolic compounds (BHM) from *Hippocampus kuda* Bleeler. *ACS Appl Mater Interfaces* 10(36):30214–30226
- [146] Li PF, Jia ZR, Wang Q, Tang PF, Wang MH, Wang KF, Fang J, Zhao CC, Ren FZ, Ge X, Lu X (2018) A resilient and flexible chitosan/silk cryogel incorporated Ag/Sr co-doped nanoscale hydroxyapatite for osteoinductivity and antibacterial properties. *J Mater Chem B* 6(45):7427–7438
- [147] Rau JV, Cacciotti I, Laureti S, Fosca M, Varvaro G, Latini A (2015) Bioactive, nanostructured Si-substituted hydroxyapatite coatings on titanium prepared by pulsed laser deposition. *J Biomed Mater Res, Part B* 103(8):1621–1631
- [148] Kezhi L, Qian G, Leilei Z, Yulei Z, Shoujie L, Kebin G, Shaoxian L (2017) Synthesis and characterization of Si-substituted hydroxyapatite bioactive coating for SiC-coated carbon/carbon composites. *Ceram Int* 43(1):1410–1414
- [149] Carlisle EM (1970) Silicon: a possible factor in bone calcification. *Science* 167(3916):279–280
- [150] Ding QQ, Zhang XJ, Huang Y, Yan YJ, Pang XF (2015) In vitro cytocompatibility and corrosion resistance of zinc-doped hydroxyapatite coatings on a titanium substrate. *J Mater Sci* 50(1):189–202. <https://doi.org/10.1007/s10853-014-8578-4>
- [151] Gao C, Li C, Wang C, Qin Y, Wang Z, Yang F, Liu H, Chang F, Wang J (2017) Advances in the induction of osteogenesis by zinc surface modification based on titanium alloy substrates for medical implants. *J Alloys Compd* 726:1072–1084
- [152] Zhu D, Cockerill I, Su Y, Zhang Z, Fu J, Lee KW, Ma J, Okpokwasili C, Tang L, Zheng Y, Qin YX, Wang Y (2019) Mechanical strength, biodegradation, and in vitro and in vivo biocompatibility of Zn biomaterials. *ACS Appl Mater Interfaces* 11(7):6809–6819
- [153] Pei L, Zhang B, Luo H, Wu X, Li G, Sheng H, Zhang L (2019) Electrodeposition of ZnO Nanoprism-Zn substituted hydroxyapatite duplex layer coating for carbon fiber. *Ceram Int* 45(11):14278–14286
- [154] Zhao HT, Tian MW, Hao YN, Qu LJ, Zhu SF, Chen SJ (2018) Fast and facile graphene oxide grafting on hydrophobic polyamide fabric via electrophoretic deposition route. *J Mater Sci* 53(13):9504–9520. <https://doi.org/10.1007/s10853-018-2230-7>
- [155] Basirun WJ, Nasiri-Tabrizi B, Baradaran S (2017) Overview of hydroxyapatite-graphene nanoplatelets composite as bone graft substitute: mechanical behavior and in vitro biofunctionality. *Crit Rev Solid State Mater Sci* 43(3):177–212
- [156] Yan Y, Zhang X, Mao H, Huang Y, Ding Q, Pang X (2015) Hydroxyapatite/gelatin functionalized graphene oxide composite coatings deposited on TiO<sub>2</sub> nanotube by electrochemical deposition for biomedical applications. *Appl Surf Sci* 329:76–82
- [157] Rodrigues BVM, Leite NCS, Cavalcanti BdN, da Silva NS, Marciano FR, Corat EJ, Webster TJ, Lobo AO (2016) Graphene oxide/multi-walled carbon nanotubes as nanofeatured scaffolds for the assisted deposition of nanohydroxyapatite: characterization and biological evaluation. *Int J Nanomed* 11:2569–2585
- [158] Zhang L, Zhu F, Li H, Zhao F, Li S (2018) A duplex coating composed of electrophoretic deposited graphene oxide inner-layer and electrodeposited graphene oxide/Mg substituted hydroxyapatite outer-layer on carbon/carbon composites for biomedical application. *Ceram Int* 44(17):21229–21237
- [159] Fathyunes L, Khalil-Allafi J (2018) The effect of graphene oxide on surface features, biological performance and biostability of calcium phosphate coating applied by pulse electrochemical deposition. *Appl Surf Sci* 437:122–135
- [160] Zeng Y, Pei X, Yang S, Qin H, Cai H, Hu S, Sui L, Wan Q, Wang J (2016) Graphene oxide/hydroxyapatite composite coatings fabricated by electrochemical deposition. *Surf Coat Technol* 286:72–79
- [161] Chakraborty R, Manna JS, Das D, Sen M, Saha P (2019) A comparative outlook of corrosion behaviour and chlorophyll assisted growth kinetics of various carbon nanostructure reinforced hydroxyapatite-calcium orthophosphate coating synthesized in situ through pulsed electrochemical deposition. *Appl Surf Sci* 475:28–42
- [162] Arul Xavier Stango S, Vijayalakshmi U (2019) Synthesis and characterization of hydroxyapatite/carboxylic acid functionalized MWCNTS composites and its triple layer coatings for biomedical applications. *Ceram Int* 45(1):69–81

- [163] Chetibi L, Achour A, Peszke J, Hamana D, Achour S (2014) Hydroxyapatite growth on multiwall carbon nanotubes grown on titanium fibers from a titanium sheet. *J Mater Sci* 49(2):621–632. <https://doi.org/10.1007/s10853-013-7742-6>
- [164] Khazeni D, Saremi M, Soltani R (2019) Development of HA-CNTs composite coating on AZ31 magnesium alloy by cathodic electrodeposition. Part 1: microstructural and mechanical characterization. *Ceram Int* 45(9):11174–11185
- [165] Chakraborty R, Seesala VS, Sen M, Sengupta S, Dhara S, Saha P, Das K, Das S (2017) MWCNT reinforced bone like calcium phosphate—Hydroxyapatite composite coating developed through pulsed electrodeposition with varying amount of apatite phase and crystallinity to promote superior osteoconduction, cytocompatibility and corrosion protection performance compared to bare metallic implant surface. *Surf Coat Technol* 325:496–514
- [166] Dziadek M, Stodolak-Zych E, Cholewa-Kowalska K (2017) Biodegradable ceramic-polymer composites for biomedical applications: a review. *Mater Sci Eng C Mater Biol Appl* 71:1175–1191
- [167] Gajendiran M, Choi J, Kim S-J, Kim K, Shin H, Koo H-J, Kim K (2017) Conductive biomaterials for tissue engineering applications. *J Ind Eng Chem* 51:12–26
- [168] Ibrahim MZ, Sarhan AAD, Yusuf F, Hamdi M (2017) Biomedical materials and techniques to improve the tribological, mechanical and biomedical properties of orthopedic implants—a review article. *J Alloys Compd* 714:636–667
- [169] Bastan FE, Atiq Ur Rehman M, Avcu YY, Avcu E, Ustel F, Boccaccini AR (2018) Electrophoretic co-deposition of PEEK-hydroxyapatite composite coatings for biomedical applications. *Colloids Surf B* 169:176–182
- [170] Zhao X, Hu T, Li H, Chen M, Cao S, Zhang L, Hou X (2011) Electrochemically assisted co-deposition of calcium phosphate/collagen coatings on carbon/carbon composites. *Appl Surf Sci* 257(8):3612–3619
- [171] Iqbal B, Sarfaraz Z, Muhammad N, Ahmad P, Iqbal J, Khan ZUH, Gonfa G, Iqbal F, Jamal A, Rahim A (2018) Ionic liquid as a potential solvent for preparation of collagen-alginate-hydroxyapatite beads as bone filler. *J Biomater Sci Polym Ed* 29(10):1168–1184
- [172] Wang J, Hidayah ZN, Abd Razak SI, Kadir MRA, Nayan NHM, Li Y, Amin KAM (2019) Surface entrapment of chitosan on 3D printed polylactic acid scaffold and its biomimetic growth of hydroxyapatite. *Compos Interfaces* 26(5):465–478
- [173] Stevanovic M, Dosic M, Jankovic A, Kojic V, Vukasinovic-Sekulic M, Stojanovic J, Odovic J, Sakase MC, Rhee KY, Miskovic-Stankovic V (2018) Gentamicin-loaded bioactive hydroxyapatite/chitosan composite coating electrodeposited on titanium. *ACS Biomater Sci Eng* 4(12):3994–4007
- [174] Molaei A, Yari M, Afshar MR (2015) Modification of electrophoretic deposition of chitosan-bioactive glass-hydroxyapatite nanocomposite coatings for orthopedic applications by changing voltage and deposition time. *Ceram Int* 41(10):14537–14544
- [175] Park KH, Kim S-J, Hwang M-J, Song H-J, Park Y-J (2017) Pulse electrodeposition of hydroxyapatite/chitosan coatings on titanium substrate for dental implant. *Colloid Polym Sci* 295(10):1843–1849
- [176] Jia L, Liang C, Huang N, Zhou Z, Duan F, Wang L (2016) Morphology and composition of coatings based on hydroxyapatite-chitosan-RuCl<sub>3</sub> system on AZ91D prepared by pulsed electrochemical deposition. *J Alloys Compd* 656:961–971
- [177] Stewart E, Kobayashi NR, Higgins MJ, Quigley AF, Jamali S, Moulton SE, Kapsa RMI, Wallace GG, Crook JM (2015) Electrical stimulation using conductive polymer polypyrrole promotes differentiation of human neural stem cells: a biocompatible platform for translational neural tissue engineering. *Tissue Eng Part C Methods* 21(4):385–393
- [178] Ning C, Zhou Z, Tan G, Zhu Y, Mao C (2018) Electroactive polymers for tissue regeneration: developments and perspectives. *Prog Polym Sci* 81:144–162
- [179] Wang F, Ju E, Guan Y, Ren J, Qu X (2017) Light-mediated reversible modulation of ROS level in living cells by using an activity-controllable nanozyme. *Small* 13(25):1603051. <https://doi.org/10.1002/sml.201603051>
- [180] Yan L, Zhao B, Liu X, Li X, Zeng C, Shi H, Xu X, Lin T, Dai L, Liu Y (2016) Aligned nanofibers from polypyrrole/graphene as electrodes for regeneration of optic nerve via electrical stimulation. *ACS Appl Mater Interfaces* 8(11):6834–6840
- [181] Shi G, Zhang Z, Rouabhia M (2008) The regulation of cell functions electrically using biodegradable polypyrrole-poly lactide conductors. *Biomaterials* 29(28):3792–3798
- [182] Madhan Kumar A, Adesina AY, Hussein MA, Ramakrishna S, Al-Aqeeli N, Akhtar S, Saravanan S (2019) PEDOT/FHA nanocomposite coatings on newly developed Ti–Nb–Zr implants: biocompatibility and surface protection against corrosion and bacterial infections. *Mater Sci Eng C* 98:482–495

**Publisher's Note** Springer Nature remains neutral with regard to jurisdictional claims in published maps and institutional affiliations.